2018-05

On the Enigma of Glutathione-Dependent Styrene Degradation in Gordonia rubripertincta CWB2

Heine, T

http://hdl.handle.net/10026.1/11849

5 ==

6

7

8 On the enigma of glutathione dependent styrene

9 degradation in *Gordonia rubripertincta* CWB2

10

11 **Thomas Heine[1,#], Juliane Zimmerling[1], Anne Ballmann[1], Sebastian Bruno**

12 **Kleeberg[1], Christian Rückert[2], Tobias Busche[2], Anika Winkler[2], Jörn**

13 **Kalinowski[2], Ansgar Poetsch[3,4], Anika Scholtissek[1], Michel Oelschlägel[1], Gert**

14 **Schmidt[5] and Dirk Tischler[1,6,#]**

15

16 [1]Institute of Biosciences, TU Bergakademie Freiberg, Leipziger Str. 29, Freiberg,

17 Germany.

18   ^{2}Technologieplattform Genomik, Centrum für Biotechnologie (CeBiTec), Universität

19   Bielefeld, Universitätsstr. 27, Bielefeld, Germany.

20   ^{3}Plant Biochemistry, Ruhr University Bochum, 44801 Bochum, Germany

21   ^{4}School of Biomedical and Healthcare Sciences, Plymouth University, Plymouth PL4

22   8AA, UK

23   ^{5}Institut für Keramik, Glas- und Baustofftechnik, TU Bergakademie Freiberg,

24   Agricolastr. 17, Freiberg, Germany.

25   ^{6}Microbial Biotechnology, Ruhr University Bochum, 44801 Bochum, Germany

26

27

28   $^#$For correspondence. E-mail heinet@tu-freiberg.de, dirk-tischler@email.de; Tel. +49

29   3731 392103.

30

31   Running title: Styrene degradation via glutathione-*S*-transferase

32

ABSTRACT

Among bacteria, only a single styrene specific degradation pathway has been reported so far. It comprises the activity of styrene monooxygenase, styrene oxide isomerase and phenylacetaldehyde dehydrogenase yielding phenylacetic acid as central metabolite. The alternative route comprises ring-hydroxylating enzymes and yields vinyl catechol as central metabolite, which undergoes *meta*-cleavage. This was reported to be unspecific and also allows the degradation of benzene derivatives. However, some bacteria had been described to degrade styrene but do not employ one of those routes or only parts of them. Herein we describe a novel "hybrid" degradation pathway for styrene located on a plasmid of foreign origin. As putatively also unspecific, it allows metabolizing chemically analogous compounds (e.g. halogenated and/or alkylated styrene derivatives). *Gordonia rubripertincta* CWB2 was isolated with styrene as sole source of carbon and energy. It employs an assembled route of the styrene side chain degradation and isoprene degradation pathways that also funnels into phenylacetic acid as central metabolite. Metabolites, enzyme activity, genome, transcriptome and proteome data reinforce the observation and allow to understand this biotechnologically relevant pathway which can be used for the production of ibuprofen.

IMPORTANCE

Degradation of xenobiotics by bacteria of high interest for bioremediation, but also as involved enzymes are potential catalysts in biotechnological applications. This study reveals a novel degradation pathway for the hazardous organic compound styrene in *Gordonia rubripertincta* CWB2. It is an impressive illustration of horizontal gene transfer, which enables novel metabolic capabilities. This study presents glutathione-dependent styrene metabolization in an (actino-)bacterium. Further, the

58 genomic background of the ability of strain CWB2 to produce ibuprofen is

59 demonstrated.

60

61 **INTRODUCTION**

62   Styrene is a monoaromatic compound that naturally occurs as a component of

63 tar, volatile and oily substances from plants and food, but can also be produced by

64 microorganisms. Styrene is of high relevance in industry and produced in million

65 tonne scale causing substantial anthropogenic release. This is problematic as it is

66 hazardous for living organisms (1–3). Due to the disposability, it is corollary that

67 organisms evolved strategies to detoxify and/or use styrene as a source of energy

68 and carbon (3–5).

69   Styrene can be channelled through different unspecific degradation pathways due

70 to relaxed substrate specificity of the respective enzymes (see supplemental material

71 and 3 for details). However, only one styrene specific degradation pathway is known

72 and seems to be favoured by microorganisms under aerobic conditions (3, 5, 6). This

73 upper degradation pathway is initiated by oxidation of the vinyl side chain. A styrene

74 monooxygenase (SMO) produces *(S)*-styrene oxide, which is converted by a

75 membrane bound styrene oxide isomerase (SOI) to phenylacetaldehyde. A

76 phenylacetaldehyde dehydrogenase (PAD) oxidizes the aldehyde to phenylacetic

77 acid (PAA) (7). PAA is a central catabolite and metabolized in the so-called lower

78 degradation pathway, which is present in about 16% of all genome-sequenced

79 microorganisms (8, 9). That route has been described for several proteobacteria

80 (*Pseudomonas*, *Xanthobacter*, *Sphingopyxis*), actinobacteria (*Rhodococcus*,

81 *Corynebacterium*) and fungi (*Exophiala*) (reviewed by 3).

82   *Rhodococcus* sp. ST-10 has an incomplete degradation cluster lacking the SOI,

83   while still being able to use styrene as sole source of carbon and energy (10–13).

84   This gene cluster comprises the SMO and a putative (partial) open reading frame

85   (ORF), designated as "ORF3". It was hypothesized that the SOI can be bypassed by

86   chemical conversion of styrene oxide to phenylacetaldehyde or enzymatically (12–

87   14). However, chemical conversion is unlikely and no probable enzymes were

88   identified (3), thus the degradation pathway for strain ST-10 remains unclear.

89   The genus *Gordonia* is known to be a versatile degrader of aromatic compounds

90   (15, 16) and *Gordonia rubripertincta* CWB2 in particular is able to metabolize styrene

91   and related compounds. As previously described, strain CWB2 was obtained from a

92   soil sample and separated via styrene-enrichment culture (17–19). Moreover, it was

93   shown that it is able to produce ibuprofen from 4-isobutyl-α-methylstyrene in a co-

94   metabolic process (17, 18). Oelschlägel *et al.* 2015 reported that other styrene

95   degraders are not capable to catalyze this reaction and therefore proposed

96   substantial differences in the respective enzymatic cascades. Interestingly, *Gordonia*

97   *rubripertincta* CWB2 has a cluster that is homolog to the partial one of strain ST-10.

98   In this study, we identified the complete gene cluster, which enables styrene

99   degradation in strain CWB2. Therefore, we studied the transcriptome and the

100   proteome under styrene exposure. Further, we measured the activity of key enzymes

101   to clarify the root of the metabolic potential of *Gordonia rubripertincta* CWB2.

102   Moreover, this gene cluster seems to be alien as it is located on a plasmid and

103   assigned as genomic island if compared to the rest of the genome. It embodies a

104   hybrid of several homolog epoxide and aromatic compound degradation clusters from

105   different actinobacteria.

106

RESULTS

Identification and annotation of gene clusters associated with styrene degradation. Genes that might be involved in styrene degradation in *G. rubripertincta* CWB2 were identified and annotated by homology search using the BLASTP algorithm (20) on the non-redundant protein database or the UniProtKB database (NCBI). The annotation of the putative styrene degradation cluster with respect to the closest (characterized) homolog is listed in Table 2 and Dataset S1. A 32424-bp cluster with 36 putative open reading frames (*orf*) was identified on the plasmid pGCWB2 (~ 100 kbp), which is framed by a styrene monooxygenase (*GCWB2_24100*) and phenylacetaldehyde dehydrogenase (*GCWB2_23925*). Interestingly, the average GC content of this cluster is 62.11% and thus 5% lower as for the whole genome. The GC content of the whole plasmid is 3% lower compared to the chromosome. Besides a high amount of hypothetical proteins, pGCWB2 contains 4 transposase-family proteins, 2 integrase-like proteins, one relaxase-like protein and one type IV secretory system as an inventory for gene mobility. Genomic island analysis on the whole genome illustrates that at least parts of this styrene degradation cluster have foreign origin (Fig. 1).

The cluster can be separated into 4 subclusters comprised as follows: cluster S1 contains a styrene monooxygenase, which is known to initiate the styrene degradation at the vinyl side chain. The closest characterized homolog of this protein was found in *Rhodococcus* sp. ST-10 (StyA – 86% identity at amino acid level; StyB – 82%). A phylogenetic analysis of the amino acid sequence classifies it as an E1-type SMO (Fig. S2). The closest match within *Gordonia* species is a putative monooxygenase from *Gordonia polyisoprenivorans* NBRC 16320 (GAB22407 – 45%; GAB22406 – 39%). However, also the genetic organisation refers to a close relation

132 to the *Rhodococcus* cluster as the partial sequence of ORF_3 from strain ST-10

133 shows 67% identity to GCWB2_24090. Transmembrane domain prediction (TMHMM)

134 of GCWB2_24090 identified 4 transmembrane helices what classifies this protein as

135 hypothetical membrane associated. Beyond that, no characterized homologs and no

136 known domains are present in the database for this ORF. It has to be mentioned that

137 no styrene oxide isomerase (*styC*) gene was found on the genome of strain CWB2.

138   The second cluster S2 embeds 7 hypothetical proteins (GCWB2_24085 -

139 GCWB2_24055). Two of them are presumably soluble and the others are annotated

140 as membrane proteins, while each has one transmembrane domain. Members of

141 these clusters appear to be rare within the database and are predominantly present

142 in rhodococci. *Rhodocoocus opacus* 1CP owns a homologous cluster downstream of

143 its StyABCD cluster (WP_065493732 - WP_045063326; 56 - 68%). Further,

144 *Gordonia* sp. i37 has a homologous gene cluster in the neighbourhood of a recently

145 recorded isoprene degradation cluster (contig257: WP_079929940 -

146 WP_079929944, contig258: OPX14963 - OPX14964; 56 - 74%) (21).

147   Cluster S3 encodes for proteins that might be involved in glutathione and

148 isoprene metabolism. GCWB2_24050 and GCWB2_24045 show highest identity to a

149 glutamate-cysteine ligase GshA (P9WPK7 – 33%) and a glutathione synthetase

150 GshB (P45480 – 50%) followed by a putative coenyzme A-disulfide reductase (CoA-

151 DSR). The other genes of this cluster (*GCWB2_24050 - GCWB2_24010*) encode for

152 a putative MarR-like transcriptional regulator, a coenzyme A-transferase, a

153 dehydrogenase, a glutathione *S*-transferase, a disulfidebond oxidoreductase and an

154 aldehyde dehydrogenase. The closest characterized homolog of the latter gene

155 product is the phenylacetaldehyde dehydrogenase from *Pseudomonas fluorescens*

156 ST (O06837 – 36%). Cluster S3 can also be found in *Aeromicrobium* sp. Root495

157   wherein a styrene monooxygenase is located between the CoA-DSR and the

158   transcriptional regulator. The same is true for *Nocardioides* sp. Root240 except for a

159   13983-bp insertion right after the styrene monooxygenase gene. Interestingly, the

160   closest characterized homologs of GCWB2_24025 and GCWB2_24020 can be found

161   in *Rhodococcus* sp. AD45 (WP_045063294 – 59%; WP_045063292 – 49%) and are

162   known to be a functional part of an isoprene degradation cluster which is located on a

163   megaplasmid (300 kbp) (22). In addition, homologs of other genes from cluster S3

164   can be found on this plasmid, even in a similar arrangement of parts from this cluster.

165   However, strain AD45 does not encode for a styrene monooxygenase on its genome

166   and on the other hand strain CWB2 is lacking the isoprene monooxygenase.

167   Homologous proteins from cluster S3 were recently found in *Gordonia* sp. i37 next to

168   a homologous to cluster S2 (21). The 13983-bp insertion of *Nocardioides* sp.

169   Root240 comprises a putative mce operon, a cluster of membrane proteins whose

170   specific function is unclear.

171   The putative styrene degradation cluster is completed by a fourth gene set S4

172   (*GCWB2_24005 - GCWB2_23925*) that encodes for proteins which are required for

173   the lower styrene degradation pathway (phenylacetic acid catabolism). The proposed

174   pathway of strain CWB2 is displayed in Figure 3b. Besides some regulatory elements

175   and a partial gene (*GCWB2_24000*), this cluster is homolog to that of *Rhodococcus*

176   *opacus* 1CP and can also be found in *Gordonia soli* NBRC 108243 as well as

177   *Gordonia* sp. i37 (contig69). The AraC-like transcriptional regulator (GCWB2_24005)

178   shows homology to regulators of strain 1CP, that are located bevor the SMO and

179   behind the PAA degradation cluster (ANS32446 – 46%; WP_061046101 – 41%).

180   However, in contrast to strain CWB2 the upper and lower styrene degradation

181   pathways are not associated in this strain. Here the genes for the conversion of

182   styrene to phenylacetic acid are located on a plasmid pR1CP1 (NZ_CP009112),

183   whereas the subsequent metabolization is encoded on the chromosome

184   (NZ_CP009111). The second transcriptional regulator (GCWB2_23980) belongs to

185   the TetR-family. Cluster S4 is terminated by a phenylacetaldehyde dehydrogenase

186   (GCWB2_23925) that is highly similar to StyD from *Rhodococcus* sp. ST-5

187   (BAL04135 – 76%). So far, a comparable genetic environment of styrene

188   monooxygenases can only be found in *Aeromicrobium* sp. Root495 and in five strains

189   of *Nocardioides* sp. (Root79, Root190, Root240, Root614, Root682). All of them were

190   isolated from *Arabidopsis* root microbiota (23).

191   As already mentioned, the whole cluster embeds 3 HTH-type regulators, which

192   are known to respond to aromatic compounds (24). They are not similar to the

193   regulation machinery as described for pseudomonads (3).

194   Besides this, the genome of strain CWB2 was examined for other genes and

195   clusters that might enable degradation of styrene or metabolites. As no styrene oxide

196   isomerase gene (*styC*) is located on the genome of strain CWB2, it might be possible

197   that this degradation step is bypassed by a styrene oxide reductase (SOR) and a

198   phenylacetaldehyde reductase (PAR). So far, there is no enzyme characterized that

199   has SOR activity and thus no comparison with strain CWB2 on DNA level is possible.

200   However, two putative ORFs (GCWB2_12345 – 70%; GCWB2_18410 – 35%) show

201   similarity to the PAR of *Rhodococcus* sp. ST-10 (BAD51480). Interestingly, the latter

202   one is part of a cluster with 8 ORFs (GCWB2_18380 - GCWB2_18415) that is

203   homolog to one in *Gordonia* sp. TY-5 (BAD03956 - BAD03963; 87 - 96%) (25). It

204   comprises a chaperonin, a putative alcohol dehydrogenase, two hypothetical proteins

205   and a putative propane monooxygenase. The monooxygenase has also resemblance

206   with a propene monooxygenase from *Mycobacterium* sp. M156 (28 - 38%) (26) but

207   also a methane monooxygenase from *Methylococcus capsulatus* Bath (29 - 34%)

208 (27). These binuclear iron monooxygenases are able to epoxidize styrene.

209 Homologous clusters can be found in several actinobacteria (28–30), for instance in

210 *R. opacus* 1CP and *Gordonia* sp. i37 (21). The other putative PAR is not part of a

211 cluster. In addition, several cytochrome P450 monooxygenases can be found on the

212 CWB2 genome, which might also be able to perform the epoxidation of styrene.

213 **Transcriptome and proteome analysis of the styrene degrader CWB2.** The

214 transcriptome and proteome of strain CWB2 was analysed to reveal the global profile

215 of genes and proteins that are involved in styrene metabolism. Therefore, fructose-

216 grown cultures served as reference condition. The transcriptome output is

217 summarized in Table S4.

218 If assuming a threshold of ≥ 1.5 (M-value), then 2.5% of the genes of strain

219 CWB2 are overexpressed under styrene exposure and 30% of these are located on

220 the plasmid (Fig. S5). It is known, that the transcriptome as the total amount of

221 mRNA does not necessarily reflect the total amount of proteins abundance in the cell.

222 However, we were able to identify 3691 proteins in the proteome of strain CWB2. If

223 assuming a threshold of 1.5 (log2 ratio), then 7% of the proteins where highly

224 abundant, when strain CWB2 was grown on styrene (Fig. S6). The gene cluster,

225 which is framed by the styrene monooxygenase and the phenylacetaldehyde

226 dehydrogenase, is highly upregulated on transcriptome (increased on average 7-fold)

227 as well as proteome level (increased on average 6.6-fold) (Table 2 and Dataset S1).

228 **Validation of enzymatic activity of selected members of the styrene**

229 **degradation pathway.** After analysis of the genome, transcriptome and proteome of

230 strain CWB2, we screened for enzyme activities that enable styrene degradation on

231 different pathways. For that, crude extract from styrene grown biomass was

232 prepared, proteins were separated and enriched by different chromatography

233   methods. The activities were measured directly or indirectly on a spectrophotometer

234   or by quantification of the products on the reverse phase HPLC (RP-HPLC),

235   respectively (Table S5). It was possible to detect SMO activity in the crude extract

236   and to enrich the enzyme 36-fold to an activity of 6.82 mU mg^{-1}. Due to the missing

237   SOI, it was proposed that the conversion of styrene oxide is bypassed by the activity

238   of a SOR, which produces 2-phenylethanol. This is supposed to be converted to

239   phenylacetaldehyde by a PAR. Only minor activity of a PAR with 2-phenylethanol

240   was detected in crude extract. Higher activities were determined in crude extracts,

241   when styrene oxide was applied as substrate. However, this might be due to activity

242   of a GST, while residual glutathione (GSH) is present in the crude extract of strain

243   CWB2. To further prove this assumption, crude extract was assayed for GST activity

244   after supply of additional GSH. Thereby, a GST activity of 44.23 U mg^{-1} was reached

245   for the conversion of styrene oxide (Fig. 2).

246   Further, crude extracts were assayed for vinylcatechol-2,3-dioxygenase and

247   *cis,cis*-muconate cycloisomerase (MCI) to exclude other degradation pathways.

248   However, there was no detectable activity for one of these enzymes.

249   Two putative SMOs of strain CWB2 were cloned and expressed for initial

250   characterization. Of the two putative SMOs, only one was expressed and synthesised

251   in an active form. It is part of the styrene degradation cluster (S1; GCWB2_24100)

252   and produces *(S)*-styrene oxide with a specific activity of 0.42 ± 0.02 U mg^{-1}. The

253   SMO can be classified as E1-type SMO (Fig. S2). PADs are aldehyde

254   dehydrogenases that catalyze the formation of the central intermediate phenylacetic

255   acid. Two aldehyde dehydrogenases of strain CWB2 were recombinantly expressed

256   in *E. coli*. Aldh1 which originates from the isoprene degradation cluster (S3) catalyzes

257   the conversion of phenylacetaldehyde with an activity of 0.29 ± 0.01 U mg^{-1}. StyD,

258   which is encoded in cluster S4 is 10-times slower and has an activity of 0.026 ± 0.001

259     $U\ mg^{-1}$.

260

261   **DISCUSSION**

262   **Adaption of *G. rubripertincta* CWB2 to styrene exposure.** Only few reports

263   exist for *Gordonia* considering the metabolization of styrene (18, 31). Further, the

264   limited amount of SMOs that are encoded on genomes of this genus indicate that

265   styrene degradation is no common feature. *Gordonia rubripertincta* CWB2 is able to

266   withstand and degrade high amounts of styrene ($520\ g\ m^{-3}$ in 21 h), even compared

267   to other efficient styrene degraders (32, 33). Some bacteria produce surfactants,

268   when they are exposed to hydrophobic substrates, to increase their accessibility (34–

269   36). However, we found no indication that strain CWB2 exports biosurfactants into

270   the media but it seems to have a hydrophobic cell surface, which improves substrate

271   uptake. This is supported by a tendency to form agglomerates during growth in liquid

272   media.

273   There is no complete prokaryotic transcriptome under styrene exposure available

274   yet. So far, studies focused on the transcriptional regulation of styrene degradation

275   and a small number of target genes, solely with respect to *Pseudomonas* strains (37–

276   44). A proteome of *R. jostii* RHA1, which employs an unspecific styrene degradation

277   route, is available (45). So far, only one system level proteome analysis for styrene

278   degradation in *P. putida* CA-3 exists (46). It was the first time where all of the

279   respective enzymes of the upper and lower degradation pathway were detected,

280   when a strain was grown on styrene (46).

281   Omic analysis of strain CWB2 in this study outlines the biological background for

282   its adaption to styrene as source of carbon and energy. This was found to be totally

283   different to so far characterized styrene degraders. Initially styrene has to be

284   imported into the cell. The only specific styrene transporter StyE was found in

285   pseudomonads (47). However, the *styE* gene is not encoded in most other styrene

286   degraders and thus, other transport mechanisms as well as diffusion have to be

287   considered (3, 46). Cluster S2 of strain CWB2 contains several membrane proteins

288   that are highly upregulated and the same cluster is also present in the styrene

289   degrader *R. opacus* 1CP (Fig. 1). Thus, it is likely that these proteins might also be

290   involved in substrate transport or cell membrane adaption. Interestingly, *Gordonia* sp.

291   i37 owns a similar cluster in proximity of an isoprene degradation cluster (21).

292   However, there are no characterized homologs available in the database and thus

293   the specific function of these proteins remains unclear.

294   **Strain CWB2 merged clusters to form a hybrid that enables styrene**

295   **degradation.** The genetic organisation of the putative styrene degradation cluster

296   compared to other clusters with homolog proteins can be found in Figure 1. The

297   "classical" styrene degradation cluster of *Pseudomonas* sp. Y2 differs to

298   *Rhodococcus* clusters as well as the recently reported cluster of *S. fribergensis* Kp5.2

299   (17, 38, 48). Thus, it is obvious that the arrangement and regulation is variable

300   among different organisms. The styrene degradation cluster of strain CWB2 is highly

301   upregulated on mRNA and protein level, when strain CWB2 grows on styrene (Table

302   2 and Dataset S1). In *Pseudomonas* putida CA-3 the SMO and PAD were the most

303   abundant proteins (46). In strain CWB2 they are also highly upregulated but in a

304   comparable range to the rest of the genes and proteins of this cluster. It can be seen

305   that the transcriptional regulators (GCWB2_24035; GCWB2_23980) are less

306   expressed and synthesized. It is also obvious that regulation of gene expression

307   differs in strain CWB2 as no StyR/StyS homolog is associated to this cluster.

308 However, further studies with different inducers are necessary to clarify the

309 regulation.

310 There is no evidence that strain CWB2 performs direct ring cleavage of styrene or

311 activation by an epoxide hydrolase as the respective parts of these pathways are not

312 present on the genome or upregulated in the transcriptome or proteome, when

313 cultivated on styrene (supplemental material). In contrast, initial epoxidation of

314 styrene was found to be catalyzed by a SMO. Enzyme activity was detected in crude

315 extracts of styrene-grown cells and the SMO was successfully enriched by ion-

316 exchange chromatography and hydrophobic interaction chromatography (Table S5).

317 The SMO (GCWB2_24100; ASR05591) was recombinantly expressed and purified.

318 The specific epoxidation activity is about 0.4 U mg^{-1} and thus higher than for most

319 other characterized SMOs (48–50). However, epoxidation of styrene is usually the

320 rate-limiting step due to the relative low activity of the SMOs (51).

321 The SMO is part of cluster S1, which is highly similar to the partial styrene

322 degradation cluster of *Rhodococcus* sp. ST-10. Toda and co-workers proposed

323 chemical conversion of styrene oxide or the cooperation of a styrene oxide reductase

324 (SOR) and phenylacetaldehyde reductase (PAR) (12, 13) as no SOI is present in this

325 strain. However, previous as well as this study indicate that this is rather unlikely, as

326 we detected only minor SOR and PAR activity in the crude extract of strain CWB2.

327 Both assumptions would not explain fast degradation of styrene as found in these

328 strains (3, 52, 53). However, strain ST-10 accumulated the epoxide when incubated

329 with styrene and thus it remains to be shown if the rest of the genes are also

330 homolog to the styrene degradation cluster in strain CWB2.

331 To circumvent this missing link of enzymatic styrene oxide isomerization, strain

332 CWB2 seems to have incorporated a cluster (S3), which is very similar to ones from

333   *Aeromicrobium* sp. Root495 and *Nocarioides* sp. Root240. Interestingly, both were

334   isolated at the same site (23) and both clusters are as well closely located to a

335   styrene monooxygenase in these strains. The genes of cluster S3 may originate from

336   an isoprene degradation cluster as found on a megaplasmid in *Rhodococcus* sp.

337   AD45 (AJ249207) but also in *Gordonia* sp. i37 (21, 54). Actinobacteria from the

338   genera *Mycobacterium*, *Rhodococcus* and *Gordonia* were constantly detected in

339   different environments as isoprene degraders (21, 54, 55). *Rhodococcus* sp. AD45

340   initially epoxidizes isoprene by the activity of an isoprene monooxygenase. Then it

341   uses a glutathione *S*-transferase to convert the epoxide to a glutathione-alcohol

342   adduct, which is further metabolized by a dehydrogenase to form an aldehyde and

343   subsequently an acid (22, 54, 56–59). Remarkably, strain AD45 is also able to

344   metabolize styrene but has no SMO (56). Derived from these observations, it might

345   be possible that styrene is also channelled through the isoprene degradation

346   pathway in *G. rubripertincta* CWB2. Further, strain CWB2 owns genes that are

347   necessary for glutathione synthesis and reduction in cluster S3 (60). Interestingly,

348   strain CWB2 does not possess an isoprene monooxygenase and has no ability to

349   catabolize isoprene (Table 1).

350   **Styrene oxide is channelled into a novel glutathione dependent degradation**

351   **pathway.** To proof, whether glutathione dependent metabolization occurs, we

352   assayed crude extract from styrene grown cells for GST activity with *(S)*-styrene

353   oxide as substrate. We found that the epoxide was degraded fast with an activity of

354   44 U mg$_{crude\ extract}^{-1}$ (Fig. 2). Only minor activity was detected when no reduced

355   glutathione was added to the reaction.

356   Therefore, we propose a novel degradation pathway for styrene via initial

357   epoxidation by a SMO to *(S)*-styrene oxide and addition of glutathione by the GST

358   StyI (Fig. 3a). The resulting *(S)*-(1-Phenyl-2-hydroxyethyl) glutathione (CAS: 64186-

359   97-6) will be further converted by the dehydrogenase StyH to *(S)*-(1-Phenyl-2-

360   acetaldehyde) glutathione and *(S)*-(1-Phenyl-2-acetic acid) glutathione. It might be

361   possible that the phenylacetaldehyde dehydrogenase (PAD) and/or the aldehyde

362   dehydrogenase (Adh1) are also involved in this step as both showed activity with

363   phenylacetaldehyde (61). As the glutathione adduct is not easily accessible it has to

364   be verified if the Adh1 and the PAD can also catalyze this reaction. It was shown that

365   the aldehyde dehydrogenase of cluster S3 are induced in strain AD45 but no specific

366   role had been ascribed (22). Subsequently the glutathione is removed from the

367   adduct what might occur by the activity of StyJ and StyG (58, 62, 63). The product of

368   this process will be phenylacetic acid or phenylacetyl-CoA, which will be degraded

369   via several enzymes from cluster S4 to yield acetyl-CoA and succinyl-CoA (Fig. 3b).

370   We suppose that the 2-phenylethanol and phenylacetaldehyde, that can be detected

371   during growth, results from side-product formation of this novel pathway due to

372   instability of the glutathione adducts or enzymatic removal of glutathione in an earlier

373   step (Fig. 3a).

374   It should be mentioned that it is unusual for actinobacteria to produce glutathione,

375   as mycothiol is the dominant thiol in these organisms (64–66). However, it was

376   reported that strain AD45 additionally produces substantial amounts of glutathione

377   and it was suggested that this ability was gained by horizontal gene transfer of

378   isoprene degradation genes (54, 56, 58, 65). It is likely that the same is true for strain

379   CWB2 due to the plasmid uptake. This is supported by the finding that the GC

380   content of the plasmid and the styrene degradation cluster is much lower compared

381   to the whole genome. The GC content of that cluster S3 is close to that of strain

382   AD45 (61.7%; (22). Recently, genes of cluster S3 were found in *Gordonia* sp. i37

383   (21). Further, strain CWB2 as well as strain 1CP encode for several mobile elements

384 in direct neighbourhood of the styrene degradation cluster on their plasmid what

385 suggests horizontal gene transfer. In addition, the cluster S4 is highly similar that that

386 of *R. opacus* 1CP and strain RHA1 and degradation of PAA likely takes place in the

387 same way (67, 68) (Fig. 3b).

388

389 **CONCLUSION**

390   Omic analyses imply that strain CWB2 incorporated a plasmid which contains an

391 assembly of different gene clusters and forms a "hybrid" that enables to metabolize

392 styrene and analogous compounds. Our study illustrates the possibilities of horizontal

393 gene transfer for Gram-positive bacteria and an ongoing adaptation to glutathione as

394 cofactor in actinobacteria. This adaption is coupled with a high biotechnological

395 potential of this organism, as *G. rubripertincta* CWB2 can produce ibuprofen, which is

396 not possible through the classical styrene degradation pathway (17, 18). The

397 involved SMO shows higher activities than reported for other SMOs so far. This might

398 be interesting as these enzymes are known to catalyze a variety of valuable reactions

399 (3). Further, bacterial GST are known to be involved in degradation of (halogenated)

400 xenobiotics and other chemical transformations and therefore the GST of strain

401 CWB2 might open a new field of possible biochemical reactions to this class of

402 enzymes (63, 69, 70).

MATERIALS AND METHODS

Isolation and cultivation of styrene-degrading strains. Styrene degrading bacteria were isolated from (contaminated) soil. A small amount of the soil was transferred into a 1-l Erlenmeyer flask and suspended in 100 ml water. Portions of 10 to 40 µl of styrene were supplied via an evaporation adaptor as sole source of carbon and energy. The growth media was dosed with 0.02 mg ml^{-1} nalidixin acid and 0.075 mg ml^{-1} cycloheximide to prevent growth of Gram-negative bacteria or fungi, respectively. 10 ml of the culture was plated on solid mineral medium (MM) (71) without carbon source and incubated at room temperature in a 5-l desiccator under styrene containing atmosphere. The grown colonies were repeatedly transferred on fresh solid mineral media and incubated for 2 - 3 days in the desiccator. The isolates were stored at - 80°C in 40% (v/v) glycerol.

Liquid cultures were kept in Erlenmeyer flasks containing mineral media (71). The respective carbon source was added either directly into the media or in case of volatile compounds via an evaporation adapter.

Characterization of *G. rubripertincta* CWB2. Growth of strain CWB2 in liquid MM was assayed on various substrates (Table S1). Production of surfactants with fructose, hexadecane or styrene as carbon source was examined as published earlier (36, 72). Siderophore production was determined by the CAS-agar plate test (73). Analysis of the mycol- and fatty acid composition was done by the Deutsche Sammlung für Mikroorganismen und Zellkulturen (DSMZ) (Table S2). 16S rRNA analysis and Scanning electron microscopy (SEM) was done as described earlier (18) (Fig. S1 and S3). The *in silico* DNA-DNA-hybridization was performed by the Genome-to-Genome Distance Calculator 2.1 (DSMZ) (Fig. S7). *G. rubripertincta*

427   CWB2 was assayed for antibiotic resistance on chloramphenicol, ampicillin,

428   tetracycline, nalidixic acid, gentamycin, streptomycin and kanamycin.

429   **DNA extraction and genome sequencing, annotation and bioinformatic**

430   **analysis.** A 50-ml culture of *G. rubripertincta* CWB2 was grown on fructose in

431   mineral media. Cells were harvested at an OD_{600} of 0.6 by centrifugation (5 000 x g;

432   15 min), washed once with 100 mM phosphate buffer (pH 7.5) and centrifuged again.

433   The cell Pellet was resuspended in 2.7 ml buffer (10 Tris-HCl, 10% sucrose, 30 mg

434   lysozyme; pH 7.8) and incubated for 1.5 h at 37°C. After centrifugation the

435   supernatant was discarded and the pellet was resuspended in 2.8 ml TE-buffer 10.1

436   (10 mM Tris, 1 mM EDTA; pH 8) with 100 µg ml^{-1} proteinase K and 150 µl

437   SDS (10%) and incubated for 2 h at 37°C. Chromosomal DNA was extracted

438   successively with 3 to 5 ml phenol (equilibrated; 2 times), phenol:chloroform:isoamyl

439   alcohol (25:24:1) and chloroform:isoamyl alcohol (24:1; 2 times). Each extraction was

440   followed by a centrifugation (20 000 x g; 10 min) and separation of the aqueous

441   phase into a new tube. Afterwards, RNA was digested by adding 100 µg ml^{-1} RNase

442   A at 37°C for 10 min. The DNA was precipitated on ice by the addition of 1/10 volume

443   of 3 M sodium acetate (pH 5.2) and 3 volumes of 100% ethanol. The precipitate was

444   centrifuged at 4°C, resuspended in 70% ice-cold ethanol and centrifuged again. The

445   supernatant was discarded and the pellet was dried for 10 min in a SpeedVac

446   vacuum concentrator. The pellet was dissolved in TE-buffer 10.1 for storage at 4°C

447   and purity was controlled by agarose-gel electrophoresis and on the Nanodrop.

448   To obtain the complete genome sequence, two sequencing libraries were

449   prepared, a TruSeq PCR-free whole genome shotgun library and a 8k Nextera

450   MatePair libary (Illumina Inc, Netherlands). Both libraries were sequenced on an

451   Illumina MiSeq desktop sequencer with 2x 300 bp. The obtained reads were

452   assembled using the Newbler (v2.8) *de novo* assembler (Roche). The initial

453   assembly consisted of just one scaffold of 90 contigs, with 120 contigs larger than

454   500 bp in total. Manual inspection and assembly was performed using CONSED (74,

455   75), which revealed a misassembly: 3 contigs representing a 105 kbp plasmid,

456   henceforth called pGCWB2, were wrongly "attached" to the scaffold representing the

457   chromosome. The sequence of both replicons could be completely established. The

458   sequences for both replicons were annotated using PROKKA (76), see Table S3 for

459   details. The annotated replicons were submitted to GenBank, the accession numbers

460   are CP022580 (chromosome) and CP022581 (pGCWB2)

461   Additional functional annotation of proteins was done by using the BLASTP

462   algorithm (20) on the non-redundant protein database or the UniProtKB database

463   (NCBI) (date of search: 01.09.2017). Membrane association of proteins was verified

464   by prediction on the TMHMM server (77). Island viewer 4 (78) was applied to detect

465   genomic islands and foreign genes on the genome of strain CWB2 (Fig. S4).

466   **RNA extraction and transcriptome sequencing.** A pre-culture of *G.*

467   *rubripertincta* CWB2 was grown at 30°C in minimal media with fructose or styrene as

468   sole source of carbon, respectively. After 5 days of cultivation the culture was diluted

469   1/10 in fresh media and incubated for 24 h with the respective substrate in a set of

470   four Erlenmeyer flasks. Prior harvesting the cells, 10% of an ice-cold STOP-solution

471   (10% buffered phenol in ethanol) was added to the culture followed by centrifugation

472   at 11 000 x g for 5 min at 4°C. The supernatant was discarded and the pellet was

473   stored until RNA isolation at - 80°C. To break up the cells, 150 µl of a 5 mg ml^{-1}

474   lysozyme solution were added to the pellet, mixed and incubated at room

475   temperature for 5 min. 450 µl of buffer RLT (Qiagen) and 50 mg of (0.1 mm) glass

476   beads were added to resuspend and break the cells by repeated vortexing at 4°C.

477 The suspension was applied to QIAshredder column for homogenization and to

478 remove particles from the sample. Extraction of total RNA Extraction was done by

479 applying the RNeasy Mini Kit including on-column DNA digestion (Qiagen). Isolated

480 RNA was stored at - 80°C and quality was controlled on the 2100 Bioanalyzer using

481 the RNA 6000 Nano Kit (Agilent).

482 RNA quality and quantity was again checked by an Agilent 2100 Bioanalyzer run

483 (Agilent Technologies, Böblingen, Germany) and Trinean Xpose sytem (Gentbrugge,

484 Belgium) prior and after rRNA depletion by Ribo-Zero rRNA Removal Kit (Bacteria)

485 (Illumina, San Diego, CA, USA). TruSeq Stranded mRNA Library Prep Kit from

486 Illumina, (San Diego, CA, USA) was used to prepare the cDNA libraries to analyze

487 the whole transcriptome. The resulting cDNAs were then sequenced paired end on

488 an Illumina MiSeq and HiSeq 1500 system (San Diego, CA, USA) using 2 x 75 nt

489 read length. The raw sequencing read files are available in the ArrayExpress

490 database (www.ebi.ac.uk/arrayexpress) under accession number: E-MTAB-6012.

491 Reads were mapped on the reference *G. rubripertincta CWB2* (CP022580,

492 CP022581) with Bowtie2 (79) using standard settings. ReadXplorer 2.2.0 (80) was

493 used for visualization of short read alignments and data analysis. Differential gene

494 expression analysis was performed based on normalized read count using TPM

495 values (Transcripts Per Million) of CDS calculated by ReadXplorer 2.2.0. The signal

496 intensity value (a-value) was calculated by 0.5*(log2 TPM condition A + log2 TPM

497 condition B) of each CDS and the signal intensity ratio (m-value) by the difference of

498 (log2) TPM. CDS with m-values of higher/equal than +1.5 or lower/equal than −1.5

499 were considered to be differentially transcribed.

500 **Preparation of protein samples and identification by LC-ESI-MS/MS mass**

501 **spectrometry.** *G. rubripertincta* CWB2 was grown the same way as for RNA

502 extraction in a set of four samples per carbon source. After cultivation, two samples

503 were pooled and centrifuged at 5 000 x g for 30 min at 4°C and resuspended in 2.5

504 ml 50 mM PP, pH 7.26. The cells were disrupted by sonication on ice (10 cycles, 1.5

505 min; power: 70%; BANDELIN Sonoplus Homogenisator HD2070) after adding 40 U

506 DNAseI and 1 mg ml^{-1} lysozyme. The suspension was centrifugated at 50 000 x g for

507 1 h at 4°C to separate soluble from insoluble matter. The proteins were separated by

508 size using discontinuous sodium dodecyl sulfate-polyacrylamide gel electrophoresis

509 (SDS-PAGE) with 50 µg of each sample per lane. Lanes were cut into 8 slices and

510 de-stained, alkylated and digested with trypsin as previously described (81, 82).

511 Peptides were extracted from the gel pieces with acetonitrile, loaded onto STAGE

512 tips for storage, and eluted from the tips shortly before MS analysis (83).

513 By using an EASY- nLC 1000 (Thermo Scientific) LC system, peptides were

514 separated at a flow rate of 400 nl/min on a 18 cm self-packed column (75 µm ID, 1.9

515 µm Reprosil-Pur 120 C-18AQ beads, Dr Maisch Germany) housed in a custom-built

516 column oven (84) at 45°C. Peptides were separated using gradient of buffers A

517 (0.1% formic acid) and B (80% acetonitrile, 0.1% formic acid) from 1% to 60% B. The

518 column was interfaced with a Nanospray Flex Ion Source (Thermo Scientific) to a Q-

519 Exactive HF mass spectrometer (Thermo Scientific). MS instrument settings were:

520 1.5 kV spray voltage, Full MS at 60K resolution, AGC target 3e6, range of 300 - 1750

521 m/z, max injection time 20 ms; Top 15 MS/MS at 15K resolution, AGC target 1e5,

522 max injection time 25 ms, isolation width 2.2 m/z, charge exclusion +1 and

523 unassigned, peptide match preferred, exclude isotope on, dynamic exclusion for 20s.

524 Mass spectra were recorded with Xcalibur software 3.1.66.10 (Thermo Scientific).

525 Using a custom database containing 4831 predicted protein sequences, proteins

526 were identified with Andromeda and quantified with the LFQ algorithm embedded in

527   MaxQuant version 1.5.3.17 (85). The following parameters were used: main search

528   max. peptide mass error of 4.5 ppm, tryptic peptides of min. 6 amino acid length with

529   max. two missed cleavages, variable oxidation of methionine, protein N-terminal

530   acetylation, fixed cysteine carbamidomethylation, LFQ min. ratio count of 2, matching

531   between runs enabled, PSM and (Razor) protein FDR of 0.01, advanced ratio

532   estimation and second peptides enabled. Proteins with a log2 ratio of higher/equal

533   than +1.5 or lower/equal than −1.5 were considered to be differentially synthesized.

534   **Cloning, expression and purification of recombinant styAs, styD and aldh1.**

535   The *styA* (*GCWB2_24100*, *GCWB2_21620*), *styD* (*GCWB2_23925*) and *aldh1*

536   (*GCWB2_24010*) genes were purchased from Eurofins MWG (Ebersberg) in a pEX-

537   K2 vector system allowing for kanamycin resistance selection. The DNA sequences

538   were optimized for the codon usage and GC content of *Acinetobacter baylyi* ADP1

539   with the OPTIMIZER tool (48, 86). 5'-NdeI and 3'-NotI restriction sites were added

540   and used for subcloning into pET16bP to obtain the expression constructs

541   pSGrA1_P01, pSGrA2_P01 and pSGrD1_P01, pSGrD2_P01 from which

542   recombinant proteins can be obtained as His_{10}-tagged proteins. *Escherichia coli*

543   strain DH5α and strain BL21 (DE3) pLysS were cultivated for cloning and expression

544   purposes as described elsewhere (87). Plasmids are listed in Table 3.

545   Expression of StyA's took place in a 3-l biofermenter. *E. coli* BL21 strains with the

546   respective plasmids were cultivated in LB media (100 µg ml^{-1} ampicillin and 50 µg ml^{-1}

547   ^{1} chloramphenicol) at 30°C until an OD_{600} of 0.4 was reached. The batch was

548   subsequently cooled to 20°C. Expression was induced at an OD_{600} of 0.6 by adding

549   0.1 mM of IPTG (isopropyl-β-$_D$-thiogalactopyranoside) to the culture and grown for 20

550   h at 20°C (120 rpm). Cells were harvested by centrifugation (5 000 x g, 30 min, 4°C),

551   resuspended in 10 mM Tris-HCl buffer (pH 7.5) and stored at - 80°C. Formation of

552 the blue dye indigo is observable if active SMOs are produced during expression in

553 LB media (88). As this was not the case for expression of *GCWB2_21620* we

554 assumed that the protein is not synthesized or active.

555   For purification of StyA, crude extracts were prepared from freshly thawed

556 biomass by disruption in a precooled French Pressure cell, followed by centrifugation

557 to remove cell debris (50 000 x g, 2 h, 4°C). The supernatants were applied to a 1-ml

558 HisTrap FF column. The column was washed with 10 CV of binding buffer (10 mM

559 Tris-HCl, 0.5 M NaCl, 25 mM imidazole, pH 7.5) to remove nonspecific bound

560 proteins. Enzymes were eluted with a linear imidazole gradient up to 500 mM over 30

561 CV. Fractions with respective enzyme activity (see 2.6.) were pooled and

562 concentrated using Sartorius Vivaspin 20 filters (5 000 MWCO) at 4°C. The

563 concentrates were passed through a 10-ml Econo-Pac 10DG desalting gravity-flow

564 column (Bio-Rad) to remove remaining imidazole and sodium chloride. Protein

565 obtained was kept in storage buffer (10 mM Tris-HCl, 50% [v/v] glycerol, pH 7.5) at -

566 20°C. Expression of *GCWB2_21620* did not yield active protein as already

567 mentioned. Preparation of StyD and Aldh1 was done according to Zimmerling *et al.*

568 2017 (61).

569   **Purification of wild-type proteins.** All following purification steps were

570 performed on an ÄKTA fast-performance liquid chromatographer (GE Healthcare).

571 Selected wild-type enzymes were enriched from crude extract by ion-exchange

572 chromatography. Therefore, strain CWB2 was cultivated on styrene and soluble

573 crude extract was prepared as described above. The supernatant was loaded with

574 buffer A (20 mM Tris-HCl; pH 7.5) on a MonoQ HR 5/5 column (GE Healthcare) at a

575 flow rate of 1 ml min^{-1}. Nonspecific bound proteins were removed by washing with 5

576 column volumes (CV) of buffer A. Elution of proteins was done over 25 CV with a

577   linear gradient of buffer B (20 mM Tris-HCl, 1 M NaCl; pH 7.5). Fractions of 1 ml were

578   collected and tested on the respective enzyme activity. A second purification step

579   was applied for some enzymes by using hydrophobic interaction chromatography.

580   Therefore, the fractions that showed the respective enzyme activity were pooled and

581     $(NH_4)_2SO_4$ was added to a final concentration of 460 mM. The sample was loaded

582   with buffer C (20 mM Tris-HCl, 0.8 M $(NH_4)_2SO_4$; pH 7.5) on a 1-ml Phenyl HP HiTrap

583   column (GE Healthcare) at a flow rate of 1 ml min^{-1}. Nonspecific bound proteins were

584   removed by washing with 5 column volumes (CV) of buffer A. Elution of proteins was

585   done over 25 CV with a linear gradient of buffer A (20 mM Tris-HCl; pH 7.5).

586   Fractions of 1 ml were tested on enzyme activity.

587   For VC12DO gel filtration was done after hydrophobic interaction

588   chromatography. Therefore, the fraction containing VC12DO activity were pooled and

589   applied with buffer D (25 mM Tris-HCl, 0.5 M NaCl; pH 7.5) to a Superdex 200 HR

590   10/30 column at a flow rate of 0.4 ml min^{-1}. Fractions of 1 ml were tested for VC12DO

591   activity.

592   Recombinant and wild-type proteins were subjected to discontinuous sodium dodecyl

593   sulfate-polyacrylamide gel electrophoresis (SDS-PAGE) (87) in order to determine

594   purity and subunit molecular size.

595   **Enzyme assays.** Crude extracts, enriched or purified protein preparations from

596   *G. rubripertincta* CWB2 were assayed for enzyme activities that are representative

597   for known degradation pathways of styrene.

598   Wild-type catechol 1,2-dioxygenase, catechol 2,3-dioxygenase and *cis,cis-*

599   muconate cycloisomerase activity was measured spectrophotometrically (Cary 50,

600   Varian) by following the product formation or substrate depletion according to

601   Warhurst *et al.* 1994 (89) using catechol, protocatechuate and *cis,cis*-muconate as

602   substrates, respectively.

603   Styrene monooxygenase (SMO) activity of wild-type and recombinant enzyme

604   preparations with styrene were measured by quantification of the reaction product

605   styrene oxide on a RP-HPLC system as described previously (90).

606   Styrene oxide reductase (SOR) and phenylacetaldehyde reductase (PAR) wild-

607   type activity with styrene oxide and 2-phenylethanol was determined by quantification

608   of the reaction products phenylacetaldehyde or 2-phenylethanol on a RP-HPLC

609   system following the protocol as described previously for the styrene oxide isomerase

610   (SOI) (17, 18).

611   Wild-type phenylacetaldehyde dehydrogenase (PAD) and wild-type PAR activity

612   was assayed indirectly on a spectrophotometer (Cary 50, Varian) by following the

613   reduction of NAD$^+$ to NADH at 340 nm (ε340 nm = 6.22 mM^{-1} cm^{-1}) (91). The 1 ml

614   assay mixture contained 0.5 mM phenylacetaldehyde or 2-phenylethanol in 10 mM

615   Tris-HCl (pH 7.5), 1 mM NAD$^+$ and 50 µl protein containing sample, respectively.

616   Recombinant PAD activity was assayed according to (61).

617   GST wild-type activity was assayed in soluble crude extract by following the *(S)*-

618   styrene oxide consumption over time. Therefore, *G. rubripertincta* CWB2 was grown

619   on MM with styrene as sole source of carbon. A 100 ml pre-culture was prepared and

620   used to inoculate the main culture 1:50 in 500 ml fresh MM. The main culture was

621   incubated at 30°C for 5 days by adding 20 to 80 µl portions styrene via gas-phase.

622   Cells were harvested by centrifugation at 5 000 x g for 20 min at 4°C. The

623   supernatant was discarded and the pellet was resuspended and washed 2 times in

624   10 ml 20 mM PP (pH 8). The cells were disrupted by sonication on ice (10 cycles,

625   1 min; power: 70%; BANDELIN Sonoplus Homogenisator HD2070) after adding 40 U

626   DNAseI and 1 mg ml^{-1} lysozyme. Soluble crude extracts were obtained by

627   centrifugation at 50 000 x g at 4°C for 1 h and separation from the insoluble matter.

628   The reaction mix (600 µl) contained 20 mM PP (pH 8), 4 mM *(S)*-styrene oxide, 5 mM

629   GSH and an appropriate amount of soluble crude extract. Blank measurements were

630   carried out by omitting either GSH or enzyme preparation. Samples were tempered

631   for 10 min at 30°C and the reaction was initiated by the addition of the substrate *(S)*-

632   styrene oxide. 25 µl samples were quenched at certain time points in 50 µl ice cold

633   acetonitrile:methanol (1:1) and centrifuged at 16 000 x g for 10 min at 4°C to remove

634   precipitates. Supernatants were applied to RP-HPLC by injection of 10 µl samples.

635   All measurements were done in triplicates. Enzyme activities are given in 1 U mg^{-1}

636   representing the conversion µmol substrate per min per mg protein.

637   All RP-HPLC measurements were done with a Eurospher C$_{18}$ column (125 mm

638   length by 4 mm i.d., 5 µm particle size, 100 Å pore size; Knauer, Germany). The

639   protein content was determined by means of the Bradford method (92), using

640   BradfordUltra reagent (Expedeon) and bovine serum albumin (Sigma) as reference

641   protein.

642   **Accession numbers.** Genome and assembly of *Gordonia rubripertincta* CWB2 is

643   deposited at NCBI (BioProject Accession: PRJNA394617; URL:

644   https://www.ncbi.nlm.nih.gov/bioproject/?term=PRJNA394617) with the chromosome

645   (CP022580) and plasmid (CP022581) sequences.

646   The raw sequencing read files are available in the ArrayExpress database

647   (www.ebi.ac.uk/arrayexpress) under accession number: E-MTAB-6012.

648   Newly characterized recombinant proteins in this study are StyA (ASR05591;

649   https://www.ncbi.nlm.nih.gov/protein/ASR05591), StyD (ASR05556;

650   https://www.ncbi.nlm.nih.gov/protein/ASR05556), Aldh1 (ASR05573;

651 https://www.ncbi.nlm.nih.gov/protein/ASR05573)   and   the   monooxygenase

652 (ASR05096; https://www.ncbi.nlm.nih.gov/protein/ASR05096).

653

659

660

661 **SUPPLEMENTAL MATERIAL**

662 Supplemental material is available at AEM's website.

663

664

REFERENCES

1. Bond JA. 1989. Review of the toxicology of styrene. Crit Rev Toxicol 19:227–249.
2. Gibbs BF, Mulligan CN. 1997. Styrene toxicity: an ecotoxicological assessment. Ecotoxicol Environ Saf 38:181–194.
3. Tischler D. 2015. Microbial styrene degradation. Springer Verlag.
4. van Agteren MH, Keuning S, Janssen DB, Janssen JP, Oosterhaven J. 2010. Handbook on biodegradation and biological treatment of hazardous organic compounds. Environment and Chemistry, v. 2. Springer Netherlands, Dordrecht.
5. Tischler D, Kaschabek SR. 2012. Microbial styrene degradation. From basics to biotechnology, 67–99. *In* Singh SN (ed), Microbial degradation of xenobiotics. Springer-Verlag, Berlin Heidelberg.
6. Mooney A, Ward PG, O'Connor KE. 2006. Microbial degradation of styrene: biochemistry, molecular genetics, and perspectives for biotechnological applications. Appl Microbiol Biotechnol 72:1–10.
7. Crabo AG, Singh B, Nguyen T, Emami S, Gassner GT, Sazinsky MH. 2017. Structure and biochemistry of phenylacetaldehyde dehydrogenase from the *Pseudomonas putida* S12 styrene catabolic pathway. Arch Biochem Biophys 616:47–58.
8. Teufel R, Mascaraque V, Ismail W, Voss M, Perera J, Eisenreich W, Haehnel W, Fuchs G. 2010. Bacterial phenylalanine and phenylacetate catabolic pathway revealed. Proc Natl Acad Sci USA 107:14390–14395.
9. Grishin AM, Cygler M. 2015. Structural organization of enzymes of the phenylacetate catabolic hybrid pathway. Biology (Basel) 4:424–442.
10. Itoh N, Yoshida K, Okada K. 1996. Isolation and identification of styrene-degrading *Corynebacterium* strains, and their styrene metabolism. Biosci Biotechnol Biochem 60:1826–1830.
11. Itoh N, Hayashi K, Okada K, Ito T, Mizuguchi N. 1997. Characterization of styrene oxide isomerase, a key enzyme of styrene and styrene oxide metabolism in *Corynebacterium* sp.. Biosci Biotechnol Biochem 61:2058–2062.
12. Itoh N, Morihama R, Wang J, Okada K, Mizuguchi N. 1997. Purification and characterization of phenylacetaldehyde reductase from a styrene-assimilating *Corynebacterium* strain, ST-10. Appl Environ Microbiol 63:3783–3788.
13. Toda H, Itoh N. 2012. Isolation and characterization of styrene metabolism genes from styrene-assimilating soil bacteria *Rhodococcus* sp. ST-5 and ST-10. J Biosci Bioeng 113:12–19.
14. Marconi AM, Beltrametti F, Bestetti G, Solinas F, Ruzzi M, Galli E, Zennaro E. 1996. Cloning and characterization of styrene catabolism genes from *Pseudomonas fluorescens* ST. Appl Environ Microbiol 62:121–127.
15. Arenskötter M, Bröker D, Steinbüchel A. 2004. Biology of the metabolically diverse genus *Gordonia*. Appl Environ Microbiol 70:3195–3204.
16. Drzyzga O. 2012. The strengths and weaknesses of *Gordonia*: a review of an emerging genus with increasing biotechnological potential. Crit Rev Microbiol 38:300–316.

709   17. Oelschlägel M, Zimmerling J, Schlömann M, Tischler D. 2014. Styrene oxide
710   isomerase of *Sphingopyxis* sp. Kp5.2. Microbiology (Reading, Engl.) 160:2481–
711   2491.
712   18. Oelschlägel M, Kaschabek SR, Zimmerling J, Schlömann M, Tischler D. 2015.
713   Co-metabolic formation of substituted phenylacetic acids by styrene-degrading
714   bacteria. Biotechnol Rep 6:20–26.
715   19. Esuola CO, Babalola OO, Heine T, Schwabe R, Schlömann M, Tischler D. 2016.
716   Identification and characterization of a FAD-dependent putrescine N-hydroxylase
717   (GorA) from *Gordonia rubripertincta* CWB2. J Mol Catal B: Enzym 134:378–389.
718   20. Altschul SF, Gish W, Miller W, Myers EW, Lipman DJ. 1990. Basic local
719   alignment search tool. J Mol Biol 215:403–410.
720   21. Johnston A, Crombie AT, El Khawand M, Sims L, Whited GM, McGenity TJ,
721   Colin Murrell J. 2017. Identification and characterisation of isoprene-degrading
722   bacteria in an estuarine environment. Environ Microbiol. doi:10.1111/1462-
723   2920.13842.
724   22. Crombie AT, Khawand ME, Rhodius VA, Fengler KA, Miller MC, Whited GM,
725   McGenity TJ, Murrell JC. 2015. Regulation of plasmid-encoded isoprene
726   metabolism in *Rhodococcus*, a representative of an important link in the global
727   isoprene cycle. Environ Microbiol 17:3314–3329.
728   23. Bai Y, Müller DB, Srinivas G, Garrido-Oter R, Potthoff E, Rott M, Dombrowski N,
729   Munch PC, Spaepen S, Remus-Emsermann M, Huttel B, McHardy AC, Vorholt
730   JA, Schulze-Lefert P. 2015. Functional overlap of the *Arabidopsis* leaf and root
731   microbiota. Nature 528:364–369.
732   24. Tropel D, van der Meer JR. 2004. Bacterial transcriptional regulators for
733   degradation pathways of aromatic compounds. Microbiol Mol Biol Rev 68:474-
734   500.
735   25. Kotani T, Yamamoto T, Yurimoto H, Sakai Y, Kato N. 2003. Propane
736   monooxygenase and NAD$^+$-dependent secondary alcohol dehydrogenase in
737   propane metabolism by *Gordonia* sp. strain TY-5. J Bacteriol 185:7120–7128.
738   26. Chan Kwo Chion CK, Askew SE, Leak DJ. 2005. Cloning, expression, and site-
739   directed mutagenesis of the propene monooxygenase genes from
740   *Mycobacterium* sp. strain M156. Appl Environ Microbiol 71:1909–1914.
741   27. Colby J, Stirling DI, Dalton H. 1977. The soluble methane monooxygenase of
742   *Methylococcus capsulatus* (Bath). Its ability to oxygenate n-alkanes, n-alkenes,
743   ethers, and alicyclic, aromatic and heterocyclic compounds. Biochem J 165:395–
744   402.
745   28. Furuya T, Hirose S, Osanai H, Semba H, Kino K. 2011. Identification of the
746   monooxygenase gene clusters responsible for the regioselective oxidation of
747   phenol to hydroquinone in mycobacteria. Appl Environ Microbiol 77:1214–1220.
748   29. Furuya T, Hayashi M, Kino K. 2013. Reconstitution of active mycobacterial
749   binuclear iron monooxygenase complex in *Escherichia coli*. Appl Environ
750   Microbiol 79:6033–6039.
751   30. Furuya T, Hayashi M, Semba H, Kino K. 2013. The mycobacterial binuclear iron
752   monooxygenases require a specific chaperonin-like protein for functional
753   expression in a heterologous host. FEBS J 280:817–826.

754   31. Narancic T, Djokic L, Kenny ST, O'Connor KE, Radulovic V, Nikodinovic-Runic J,
755   Vasiljevic B. 2012. Metabolic versatility of Gram-positive microbial isolates from
756   contaminated river sediments. J Hazard Mater 215-216:243–251.

757   32. Braun-Lüllemann A, Majcherczyk A, Hüttermann A. 1997. Degradation of styrene
758   by white-rot fungi. Appl Microbiol Biotechnol 47:150–155.

759   33. Gaszczak A, Bartelmus G, Gren I. 2012. Kinetics of styrene biodegradation by
760   *Pseudomonas* sp. E-93486. Appl Microbiol Biotechnol 93:565–573.

761   34. Bredholt H, Josefsen K, Vatland A, Bruheim P, Eimhjellen K. 1998.
762   Emulsification of crude oil by an alkane-oxidizing *Rhodococcus* species isolated
763   from seawater. Can J Microbiol 44:330–340.

764   35. Lang S, Philp JC. 1998. Surface-active lipids in rhodococci. Antonie Van
765   Leeuwenhoek 74:59–70.

766   36. Franzetti A, Bestetti G, Caredda P, La Colla P, Tamburini E. 2008. Surface-
767   active compounds and their role in the access to hydrocarbons in *Gordonia*
768   strains. FEMS Microbiol Ecol 63:238–248.

769   37. O'Connor K, Buckley CM, Hartmans S, Dobson AD. 1995. Possible regulatory
770   role for nonaromatic carbon sources in styrene degradation by *Pseudomonas*
771   *putida* CA-3. Appl Environ Microbiol 61:544–548.

772   38. Velasco A, Alonso S, Garcia JL, Perera J, Diaz E. 1998. Genetic and functional
773   analysis of the styrene catabolic cluster of *Pseudomonas* sp. strain Y2. J
774   Bacteriol 180:1063–1071.

775   39. Santos PM, Blatny JM, Di Bartolo I, Valla S, Zennaro E. 2000. Physiological
776   analysis of the expression of the styrene degradation gene cluster in
777   *Pseudomonas fluorescens* ST. Appl Environ Microbiol 66:1305–1310.
778   doi:10.1128/AEM.66.4.1305-1310.2000.

779   40. O'Leary ND, O'Connor KE, Duetz W, Dobson AD. 2001. Transcriptional
780   regulation of styrene degradation in *Pseudomonas putida* CA-3. Microbiology
781   (Reading, Engl.) 147:973–979.

782   41. Leoni L, Ascenzi P, Bocedi A, Rampioni G, Castellini L, Zennaro E. 2003.
783   Styrene-catabolism regulation in *Pseudomonas fluorescens* ST: phosphorylation
784   of StyR induces dimerization and cooperative DNA-binding. Biochem Biophys
785   Res Commun 303:926–931.

786   42. Leoni L, Rampioni G, Di Stefano V, Zennaro E. 2005. Dual role of response
787   regulator StyR in styrene catabolism regulation. Appl Environ Microbiol 71:5411–
788   5419.

789   43. Milani M, Leoni L, Rampioni G, Zennaro E, Ascenzi P, Bolognesi M. 2005. An
790   active-like structure in the unphosphorylated StyR response regulator suggests a
791   phosphorylation-dependent allosteric activation mechanism. Structure 13:1289–
792   1297.

793   44. del Peso-Santos T, Shingler V, Perera J. 2008. The styrene-responsive
794   StyS/StyR regulation system controls expression of an auxiliary phenylacetyl-
795   coenzyme A ligase. Implications for rapid metabolic coupling of the styrene
796   upper- and lower-degradative pathways. Mol Microbiol 69:317–330.

797   45. Patrauchan MA, Florizone C, Eapen S, Gomez-Gil L, Sethuraman B, Fukuda M,
798   Davies J, Mohn WW, Eltis LD. 2008. Roles of ring-hydroxylating dioxygenases in

799   styrene and benzene catabolism in *Rhodococcus jostii* RHA1. J Bacteriol
800   190:37–47.
801   46. Nikodinovic-Runic J, Flanagan M, Hume AR, Cagney G, O'Connor KE. 2009.
802   Analysis of the *Pseudomonas putida* CA-3 proteome during growth on styrene
803   under nitrogen-limiting and non-limiting conditions. Microbiology (Reading, Engl.)
804   155:3348–3361.
805   47. Mooney A, O'Leary ND, Dobson ADW. 2006. Cloning and functional
806   characterization of the styE gene, involved in styrene transport in *Pseudomonas
807   putida* CA-3. Appl Environ Microbiol 72:1302–1309. doi:10.1128/AEM.72.2.1302-
808   1309.2006.
809   48. Riedel A, Heine T, Westphal AH, Conrad C, Rathsack P, van Berkel WJH,
810   Tischler D. 2015. Catalytic and hydrodynamic properties of styrene
811   monooxygenases from *Rhodococcus opacus* 1CP are modulated by cofactor
812   binding. AMB Express 5:112.
813   49. Otto K, Hofstetter K, Röthlisberger M, Witholt B, Schmid A. 2004. Biochemical
814   characterization of StyAB from *Pseudomonas* sp. strain VLB120 as a two-
815   component flavin-diffusible monooxygenase. J Bacteriol 186:5292–5302.
816   50. Toda H, Imae R, Komio T, Itoh N. 2012. Expression and characterization of
817   styrene monooxygenases of *Rhodococcus* sp. ST-5 and ST-10 for synthesizing
818   enantiopure (*S*)-epoxides. Appl Microbiol Biotechnol 96:407–418.
819   51. Cheng L, Yin S, Chen M, Sun B, Hao S, Wang C. 2016. Enhancing indigo
820   production by over-expression of the styrene monooxygenase in *Pseudomonas
821   putida*. Curr Microbiol 73:248–254.
822   52. Han JH, Park MS, Bae JW, Lee EY, Yoon YJ, Lee S-G, Park S. 2006. Production
823   of (*S*)-styrene oxide using styrene oxide isomerase negative mutant of
824   *Pseudomonas putida* SN1. Enzyme Microb Technol 39:1264–1269.
825   53. Oelschlägel M, Gröning JAD, Tischler D, Kaschabek SR, Schlömann M. 2012.
826   Styrene oxide isomerase of *Rhodococcus opacus* 1CP, a highly stable and
827   considerably active enzyme. Appl Environ Microbiol 78:4330–4337.
828   54. El Khawand M, Crombie AT, Johnston A, Vavlline DV, McAuliffe JC, Latone JA,
829   Primak YA, Lee S-K, Whited GM, McGenity TJ, Murrell JC. 2016. Isolation of
830   isoprene degrading bacteria from soils, development of *isoA* gene probes and
831   identification of the active isoprene-degrading soil community using DNA-stable
832   isotope probing. Environ Microbiol 18:2743–2753.
833   55. Alvarez LA, Exton DA, Timmis KN, Suggett DJ, McGenity TJ. 2009.
834   Characterization of marine isoprene-degrading communities. Environ Microbiol
835   11:3280–3291.
836   56. van Hylckama VJ, Kingma J, van den Wijngaard, A J, Janssen DB. 1998. A
837   glutathione *S*-transferase with activity towards cis-1,2-dichloroepoxyethane is
838   involved in isoprene utilization by *Rhodococcus* sp. strain AD45. Appl Environ
839   Microbiol 64:2800–2805.
840   57. van Hylckama VJ, Kingma J, Kruizinga W, Janssen DB. 1999. Purification of a
841   glutathione *S*-transferase and a glutathione conjugate-specific dehydrogenase
842   involved in isoprene metabolism in *Rhodococcus* sp. strain AD45. J Bacteriol
843   181:2094–2101.

844 58. van Hylckama VJ, Leemhuis H, Spelberg JHL, Janssen DB, Spelberg JH, van
845 Hylckama Vlieg JE. 2000. Characterization of the gene cluster involved in
846 isoprene metabolism in *Rhodococcus* sp. strain AD45. J Bacteriol 182:1956–
847 1963.
848 59. El Khawand M. 2014. Bacterial degradation of isoprene in the terrestrial
849 environment. Dissertation. University of East Anglia, Norwich.
850 60. Smirnova GV, Oktyabrsky ON. 2005. Glutathione in bacteria. Biochem (Moscow)
851 70:1199–1211.
852 61. Zimmerling J, Tischler D, Grossmann C, Schlömann M, Oelschlägel M. 2017.
853 Characterization of aldehyde dehydrogenases applying an enzyme assay with *in*
854 *situ* formation of phenylacetaldehydes. Appl Biochem Biotechnol:1–13.
855 62. Fall R, Copley SD. 2000. Bacterial sources and sinks of isoprene, a reactive
856 atmospheric hydrocarbon. Environ Microbiol 2:123–130.
857 63. Allocati N, Federici L, Masulli M, Di Ilio C. 2009. Glutathione transferases in
858 bacteria. FEBS J 276:58–75.
859 64. Fahey RC, Brown WC, Adams WB, Worsham MB. 1978. Occurrence of
860 glutathione in bacteria. J Bacteriol 133:1126–1129.
861 65. Johnson T, Newton GL, Fahey RC, Rawat M. 2009. Unusual production of
862 glutathione in Actinobacteria. Arch Microbiol 191:89–93.
863 66. Allocati N, Federici L, Masulli M, Di Ilio C. 2012. Distribution of glutathione
864 transferases in Gram-positive bacteria and Archaea. Biochimie 94:588–596.
865 67. Navarro-Llorens JM, Patrauchan MA, Stewart GR, Davies JE, Eltis LD, Mohn
866 WW. 2005. Phenylacetate catabolism in *Rhodococcus* sp. strain RHA1: a central
867 pathway for degradation of aromatic compounds. J Bacteriol 187:4497–4504.
868 68. Chen X, Kohl TA, Rückert C, Rodionov DA, Li L-H, Ding J-Y, Kalinowski J, Liu S-
869 J. 2012. Phenylacetic acid catabolism and its transcriptional regulation in
870 *Corynebacterium glutamicum*. Appl Environ Microbiol 78:5796–5804.
871 69. van Hylckama VJ, Janssen DB. 2001. Formation and detoxification of reactive
872 intermediates in the metabolism of chlorinated ethenes. J Biotechnol 85:81–102.
873 70. Rui L, Kwon YM, Reardon KF, Wood TK. 2004. Metabolic pathway engineering
874 to enhance aerobic degradation of chlorinated ethenes and to reduce their
875 toxicity by cloning a novel glutathione *S*-transferase, an evolved toluene o-
876 monooxygenase, and gamma-glutamylcysteine synthetase. Environ Microbiol
877 6:491–500.
878 71. Dorn E, Hellwig M, Reineke W, Knackmuss H-J. 1974. Isolation and
879 characterization of a 3-chlorobenzoate degrading pseudomonad. Arch Microbiol
880 99:61–70.
881 72. Cooper DG, Goldenberg BG. 1987. Surface-active agents from two bacillus
882 species. Appl Environ Microbiol 53:224–229.
883 73. Ames-Gottfred NP, Christie BR, Jordan DC. 1989. Use of the Chrome Azurol S
884 agar plate technique to differentiate strains and field isolates of *Rhizobium*
885 *leguminosarum* biovar *trifolii*. Appl Environ Microbiol 55:707–710.
886 74. Gordon D, Abajian C, Green P. 1998. Consed: a graphical tool for sequence
887 finishing. Genome Res 8:195–202.
888 75. Gordon D, Green P. 2013. Consed. A graphical editor for next-generation
889 sequencing. Bioinformatics 29:2936–2937.

890 76. Seemann T. 2014. Prokka: rapid prokaryotic genome annotation. Bioinformatics
891   30:2068–2069.
892 77. Krogh A, Larsson B, Heijne G von, Sonnhammer EL. 2001. Predicting
893   transmembrane protein topology with a hidden Markov model: application to
894   complete genomes. J Mol Biol 305:567–580.
895 78. Bertelli C, Laird MR, Williams KP, Lau BY, Hoad G, Winsor GL, Brinkman FS.
896   2017. IslandViewer 4. Expanded prediction of genomic islands for larger-scale
897   datasets. Nucleic Acids Res. doi:10.1093/nar/gkx343.
898 79. Langmead B, Salzberg SL. 2012. Fast gapped-read alignment with Bowtie 2. Nat
899   Methods 9:357–359.
900 80. Hilker R, Stadermann KB, Schwengers O, Anisiforov E, Jaenicke S, Weisshaar
901   B, Zimmermann T, Goesmann A. 2016. ReadXplorer 2-detailed read mapping
902   analysis and visualization from one single source. Bioinformatics 32:3702–3708.
903 81. Shevchenko A, Tomas H, Havlis J, Olsen JV, Mann M. 2006. In-gel digestion for
904   mass spectrometric characterization of proteins and proteomes. Nat Protoc
905   1:2856–2860.
906 82. Al-Furoukh N, Ianni A, Nolte H, Hölper S, Krüger M, Wanrooij S, Braun T. 2015.
907   ClpX stimulates the mitochondrial unfolded protein response (UPRmt) in
908   mammalian cells. Biochim Biophys Acta 1853:2580–2591.
909 83. Rappsilber J, Mann M, Ishihama Y. 2007. Protocol for micro-purification,
910   enrichment, pre-fractionation and storage of peptides for proteomics using
911   StageTips. Nat Protoc 2:1896–1906.
912 84. Thakur SS, Geiger T, Chatterjee B, Bandilla P, Fröhlich F, Cox J, Mann M. 2011.
913   Deep and highly sensitive proteome coverage by LC-MS/MS without
914   prefractionation. Mol Cell Proteomics 10:M110.003699.
915 85. Cox J, Hein MY, Luber CA, Paron I, Nagaraj N, Mann M. 2014. Accurate
916   proteome-wide label-free quantification by delayed normalization and maximal
917   peptide ratio extraction, termed MaxLFQ. Mol Cell Proteomics 13:2513–2526.
918 86. Puigbo P, Guzman E, Romeu A, Garcia-Vallve S. 2007. OPTIMIZER: a web
919   server for optimizing the codon usage of DNA sequences. Nucleic Acids Res
920   35:W126-W131.
921 87. Sambrook J, Russell DW (ed.). 2001. Molecular cloning. A laboratory manual,
922   3rd ed. Cold Spring Harbor Laboratory Press, Cold Spring Harbor, NY.
923 88. O'Connor KE, Dobson AD, Hartmans S. 1997. Indigo formation by
924   microorganisms expressing styrene monooxygenase activity. Appl Environ
925   Microbiol 63:4287–4291.
926 89. Warhurst AM, Clarke KF, Hill RA, Holt RA, Fewson CA. 1994. Metabolism of
927   styrene by *Rhodococcus rhodochrous* NCIMB 13259. Appl Environ Microbiol
928   60:1137–1145.
929 90. Tischler D, Eulberg D, Lakner S, Kaschabek SR, van Berkel WJH, Schlömann M.
930   2009. Identification of a novel self-sufficient styrene monooxygenase from
931   *Rhodococcus opacus* 1CP. J Bacteriol 191:4996–5009.
932 91. Dawson, R. M. C. 1986. Data for biochemical research, 3rd ed. Clarendon Press,
933   Oxford.
934 92. Bradford MM. 1976. A rapid and sensitive method for the quantitation of
935   microgram quantities of protein utilizing the principle of protein-dye binding. Anal
936   Biochem 72:248–254.
937 93. Alonso S, Bartolomé-Martín D, del Álamo M, Díaz E, García JL, Perera J. 2003.
938   Genetic characterization of the styrene lower catabolic pathway of *Pseudomonas*
939   sp. strain Y2. Gene 319:71–83.

940 94. El-Said Mohamed M. 2000. Biochemical and molecular characterization of
941 phenylacetate-coenzyme A ligase, an enzyme catalyzing the first step in aerobic
942 metabolism of phenylacetic acid in *Azoarcus evansii*. J Bacteriol 182:286–294.

943 95. Kendall SL, Burgess P, Balhana R, Withers M, Bokum A ten, Lott JS, Gao C,
944 Uhia-Castro I, Stoker NG. 2010. Cholesterol utilization in mycobacteria is
945 controlled by two TetR-type transcriptional regulators: kstR and kstR2.
946 Microbiology (Reading, Engl.) 156:1362–1371.

947 96. Nagy I, Schoofs G, Compernolle F, Proost P, Vanderleyden J, Mot R de. 1995.
948 Degradation of the thiocarbamate herbicide EPTC (*S*-ethyl
949 dipropylcarbamothioate) and biosafening by *Rhodococcus* sp. strain NI86/21
950 involve an inducible cytochrome P-450 system and aldehyde dehydrogenase. J
951 Bacteriol 177:676–687.

952 97. Takeo M, Murakami M, Niihara S, Yamamoto K, Nishimura M, Kato D-i, Negoro
953 S. 2008. Mechanism of 4-nitrophenol oxidation in *Rhodococcus* sp. strain PN1:
954 characterization of the two-component 4-nitrophenol hydroxylase and regulation
955 of its expression. J Bacteriol 190:7367–7374.

956 98. Beltrametti F, Marconi AM, Bestetti G, Colombo C, Galli E, Ruzzi M, Zennaro E.
957 1997. Sequencing and functional analysis of styrene catabolism genes from
958 *Pseudomonas fluorescens* ST. Appl Environ Microbiol 63:2232–2239.

959 99. Wadington MC, Ladner JE, Stourman NV, Harp JM, Armstrong RN. 2009.
960 Analysis of the structure and function of YfcG *from Escherichia coli* reveals an
961 efficient and unique disulfide bond reductase. Biochem 48:6559–6561.

962 100. Mullins EA, Sullivan KL, Kappock TJ. 2013. Function and X-ray crystal
963 structure of *Escherichia coli* YfdE. PLoS One 8:e67901.

964 101. Reverchon S, Nasser W, Robert-Baudouy J. 1994. pecS: a locus controlling
965 pectinase, cellulase and blue pigment production in *Erwinia chrysanthemi*. Mol
966 Microbiol 11:1127–1139.

967 102. Harris DR, Ward DE, Feasel JM, Lancaster KM, Murphy RD, Mallet TC, Crane
968 EJ3. 2005. Discovery and characterization of a Coenzyme A disulfide reductase
969 from *Pyrococcus horikoshii*. Implications for this disulfide metabolism of
970 anaerobic hyperthermophiles. FEBS J 272:1189–1200.

971 103. Zhang CC, Huguenin S, Friry A. 1995. Analysis of genes encoding the cell
972 division protein FtsZ and a glutathione synthetase homologue in the
973 cyanobacterium Anabaena sp. PCC 7120. Res Microbiol 146:445–455.

974 104. Harth G, Maslesa-Galic S, Tullius MV, Horwitz MA. 2005. All four
975 *Mycobacterium tuberculosis* glnA genes encode glutamine synthetase activities
976 but only GlnA1 is abundantly expressed and essential for bacterial homeostasis.
977 Mol Microbiol 58:1157–1172.

978 105. Gupta RS. 1994. Identification of a GroES (CPN10)-related sequence motif in
979 the GroEL (CPN60) chaperonins. Biochem Mol Biol Int 33:591–595.

980 106. Hahn J-S, Oh S-Y, Roe J-H. 2002. Role of OxyR as a peroxide-sensing
981 positive regulator in *Streptomyces coelicolor* A3(2). J Bacteriol 184:5214–5222.

982 107. Dhandayuthapani S, Zhang Y, Mudd MH, Deretic V. 1996. Oxidative stress
983 response and its role in sensitivity to isoniazid in mycobacteria: characterization
984 and inducibility of ahpC by peroxides in *Mycobacterium smegmatis* and lack of
985 expression in *M. aurum* and *M. tuberculosis*. J Bacteriol 178:3641–3649.

986 108. Ramachandran S, Magnuson TS, Crawford DL. 2000. Isolation and analysis of
987 three peroxide sensor regulatory gene homologs ahpC, ahpX and oxyR in
988 *Streptomyces viridosporus* T7A--a lignocellulose degrading actinomycete. DNA
989 Seq 11:51–60.

990

FIGURE LEGENDS

992 **Fig. 1.** Comparison of the styrene degradation cluster of *Gordonia rubripertincta*
993 CWB2 with homologous clusters as found in the strains *Rhodococcus opacus* PD630
994 (Accession: NZ_CP003949) (22), *Rhodococcus* sp. AD45 (NZ_CM003191) (58),
995 *Nocardioides* sp. Root240 (NZ_LMIT01000013), *Aeromicrobium* sp. Root495
996 (NZ_LMFJ01000002), *Rhodococcus* sp. ST-10 (AB594506) (13), *Rhodococcus*
997 *opacus* 1CP (NZ_CP009112, NZ_CP009111) (48), *Pseudomonas* sp. Y2 (AJ000330)
998 (38, 93) and *Sphingopyxis fribergensis* sp. Kp5.2 (CP009122) (17). Subclusters of
999 strain CWB2 are indicated (S1-S4) and gene products are given in the legend
1000 coloured by their (predicted) function. Relevant homologous genes and clusters are
1001 emphasized by interspaced conjunctions. Clusteres of marked strains are reported to
1002 be involved in isoprene (●) or styrene (♯) degradation.

1003 **Fig. 2.** Degradation of 4 mM *(S)*-styrene oxide with crude extract of styrene grown
1004 biomass of *Gordonia rubripertincta* CWB2 and 5 mM reduced glutathione (●). Only
1005 minor consumption was detected when excluding either reduced glutathione (○) or
1006 crude extract (X) from the reaction mix.

1007 **Fig. 3a.** Proposed novel degradation pathway of styrene in *Gordonia rubripertincta*
1008 CWB2 (see text for details). **3b.** Proposed phenylacetic acid degradation pathway of
1009 *Gordonia rubripertincta* CWB2. The genes of the involved enzymes are present on
1010 the genome (cluster S4) and upregulated on transcriptome and the proteins on
1011 proteome level, respectively (see Table 2). Starting from the product of the upper
1012 degradation pathway, phenylacetic acid, strain CWB2 is able to metabolize styrene to
1013 acetyl-CoA or succinyl-CoA (adapted to 68).

TABLE LEGENDS

Table 1. Substrate spectra with focus on ones that might be related to styrene degradation in *G. rubripertincta* CWB2.

Table 2. Functional categorization of proteins from *G. rubripertincta* CWB2 that are supposed to be involved in styrene degradation and regulation on RNA and protein level. Enzymes and proteins with reported activity or function are underlined. For further details, see Dataset S1 in supporting material.

Table 3. Plasmids used in this study.
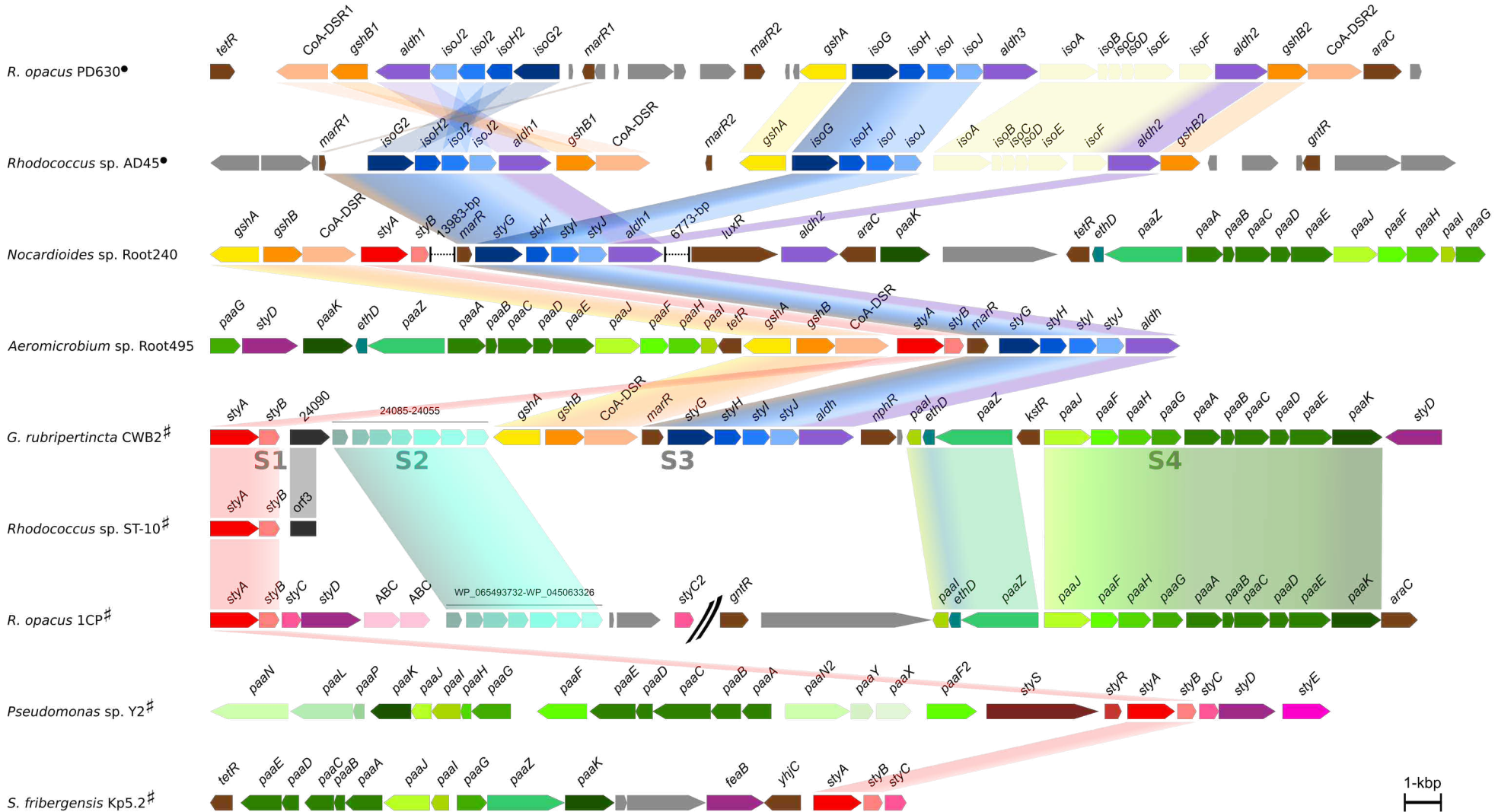
Legend:

Styrene monooxygenase	Glutamate cysteine ligase
Styrene oxide isomerase	Glutathione synthetase
Phenylacetaldehyde dehydrogenase	CoA-disulfide reductase
Sensor kinase	CoA-transferase
Response regulator	Dehydrogenase
ATPase-like transporter	Glutathione-*S*-transferase
Aldehyde dehydrogenase	Glutathione-*S*-transferase

1,2-phenylacetyl-CoA epoxidase	Phenylacetate permease
2,3-dehydroadipyl-CoA hydratase	Ring opening enzyme
1,2-epoxyphenylacetyl-CoA isomerase	Membrane protein
3-hydroxyadipyl-CoA dehydrogenase	Transcriptional repressor
Acyl-CoA thioesterase	Regulator
3-oxoadipyl-CoA/3-oxo-5,6-dehydrosuberyl-CoA thiolase	Bifunctional dehydrogenase/hydratase
Phenylacetate-CoA ligase	Ethyl *tert*-butyl ether protein

Isoprene monooxygenase	
Transcriptional regulator	
ABC Transporter	
Hypothetical protein	

3a. Upper degradation pathway
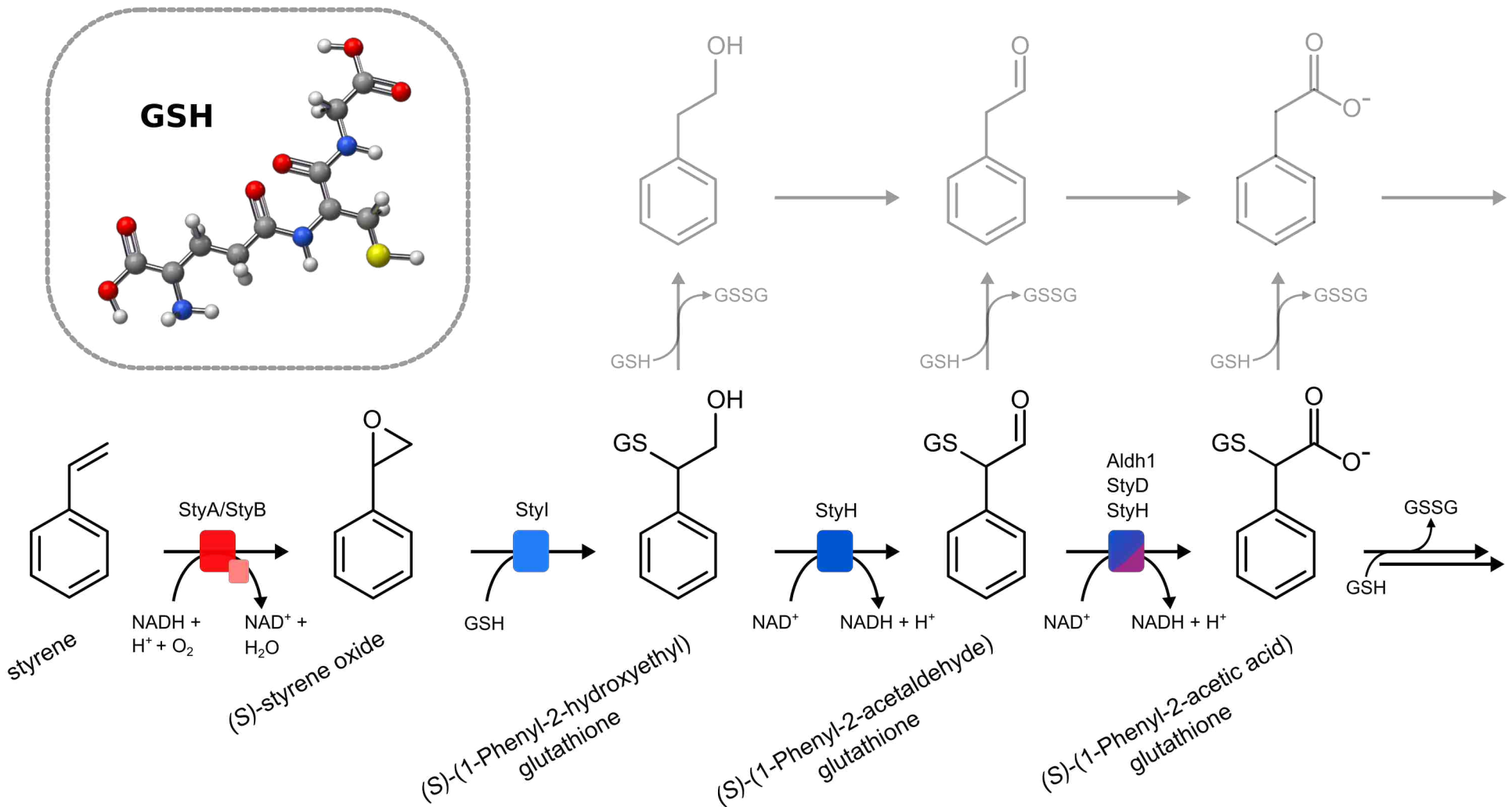
3b. Lower degradation pathway

Table 1. Substrate spectra with focus on ones that might be related to styrene degradation in *G. rubripertincta* CWB2.

Substrate	Utilization
Styrene	++
Styrene oxide	++
2-Phenylethanol	++
Phenylacetaldehyde	++
Phenylacetic acid	+++
Succinate	++
Citrate	++
Isoprene	-
Mandelic acid	-
D-Fructose	+++

(+++) vigorous growth; (++) good growth; (+) growth; (-) no growth

Table 2. Functional categorization of proteins from *G. rubripertincta* CWB2 that are supposed to be involved in styrene degradation and regulation on RNA and protein level. Enzymes and proteins with reported activity or function are underlined. For further details see supporting information.

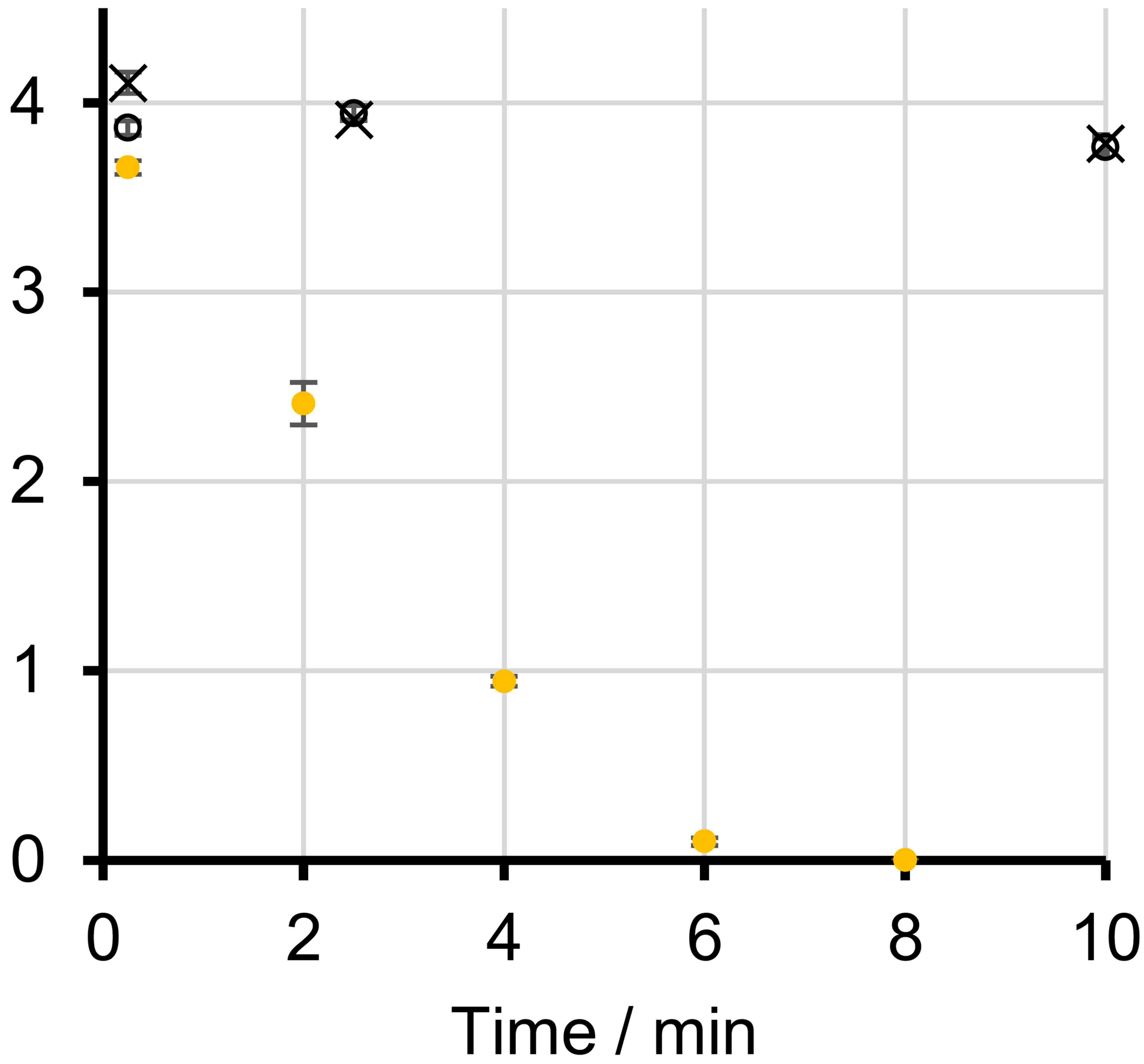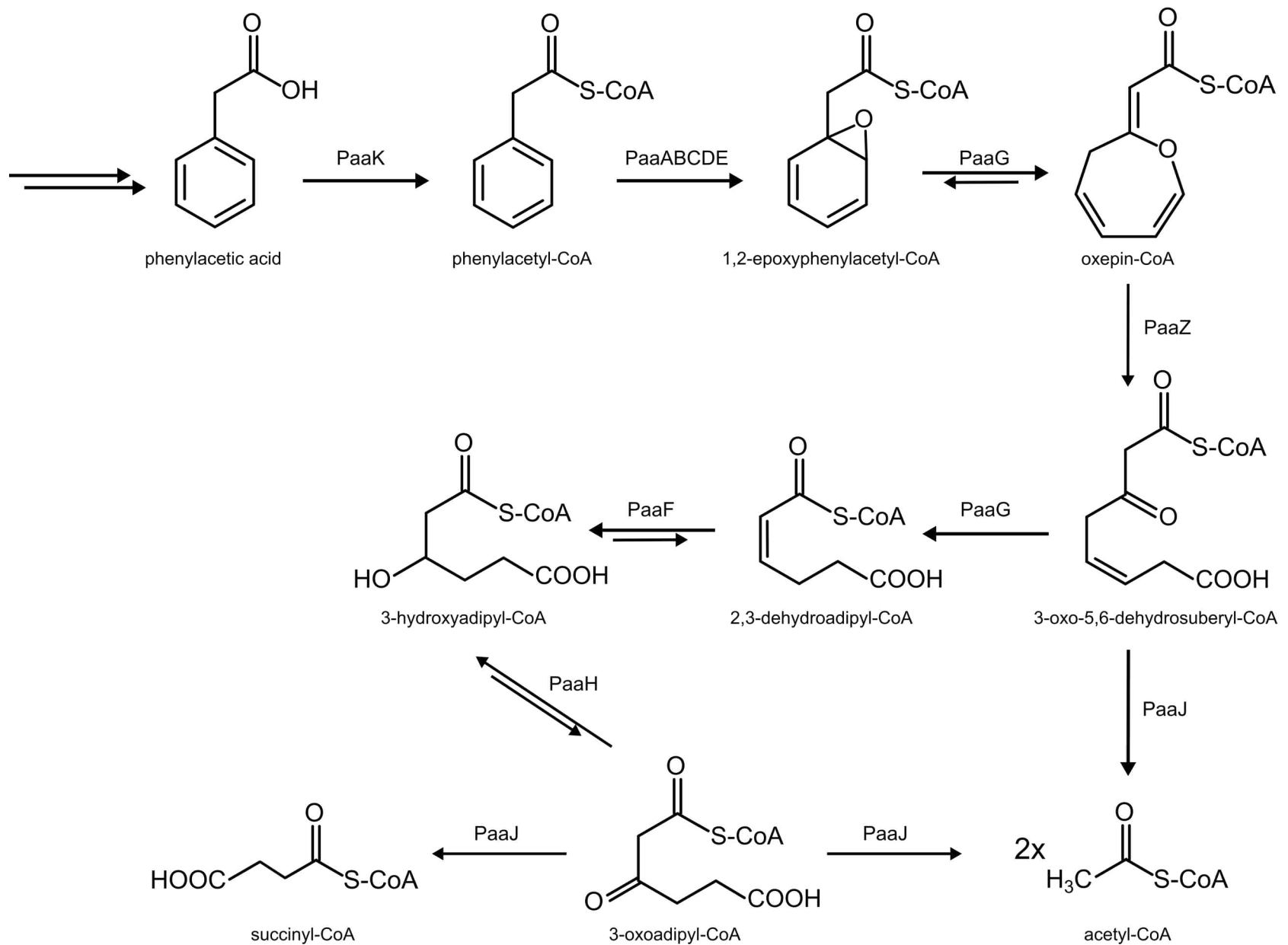|		Transcriptome		Proteome			Best hit on the Uniprot Database at amino acid level				
ORF	Gene	A	M	Cyt	Mem		Name*	Function	Accession	% Id	Reference
23925	*styD*	7.7	8.6	7.1	5.7		*styD*	Phenylacetaldehyde dehydrogenase	BAL04135	76	(13, 50)
23930	*paaK*	8.1	6.0	8.1	5.9		*paaK*	Phenylacetate-coenzyme A ligase	Q9L9C1	68	(94)
23935	*paaE*	8.0	6.2	11.3	8.2		*paaE*	1,2-phenylacetyl-CoA epoxidase, subunit E	P76081	43	(8)
23940	*paaD*	8.1	6.7	NaNf	NaNf		*paaD*	1,2-phenylacetyl-CoA epoxidase, subunit D	P76080	42	(8)
23945	*paaC*	8.3	6.7	10.5	7.4		*paaC*	1,2-phenylacetyl-CoA epoxidase, subunit C	P76079	42	(8)
23950	*paaB*	8.0	6.8	8.8	9.1		*paaB*	1,2-phenylacetyl-CoA epoxidase, subunit B	P76078	67	(8)
23955	*paaA*	8.5	7.1	11.4	9.0		*paaA*	1,2-phenylacetyl-CoA epoxidase, subunit A	P76077	66	(8)
23960	*paaG*	7.7	7.4	6.9	6.8		*paaG*	1,2-epoxyphenylacetyl-CoA isomerase	P77467	37	(8)
23965	*paaH*	7.6	7.5	7.1	6.2	S4	*paaH*	3-hydroxyadipyl-CoA dehydrogenase	P76083	36	(8)
23970	*paaF*	7.1	7.4	7.1	5.8		*paaF*	2,3-dehydroadipyl-CoA hydratase	P76082	36	(8)
23975	*paaJ*	6.6	8.2	7.4	6.6		*paaJ*	3-oxoadipyl-CoA/3-oxo-5,6-dehydrosuberyl-CoA thiolase	P0C7L2	55	(8)
23980	*tetR*	7.3	1.8	2.7	1.8		*kstR2*	HTH-type transcriptional repressor KstR2	A0R4Z6	25	(95)
23985	*paaZ*	7.9	6.4	6.8	6.0		*paaZ*	bifunctional aldehyde dehydrogenase	P77455	51	(8)
23990	*ethD*	8.4	6.3	5.1	5.7		*ethD*	Uncharacterized 11.0 kDa protein	P43491	48	(96)
23995	*paaI*	7.3	5.2	NaNf	NaNf		*paaI*	Acyl-coenzyme A thioesterase PaaI	P76084	45	(8)
24000	partial	7.3	6.4	NaN	NaN		-	-	-	-	-
24005	*araC*	8.0	6.0	4.1	8.4		*nphR*	Transcriptional activator NphR	B1Q2A8	31	(97)
24010	*aldh1*	9.6	6.4	6.0	5.5		*styD*	Phenylacetaldehyde dehydrogenase	O06837	36	(98)
24015	*styJ*	10.1	6.1	7.7	5.9		*yfcG*	Disulfide-bond oxidoreductase YfcG	P77526	47	(99)
24020	*styI*	10.4	6.0	5.0	5.3		*isoI*	Glutathione-*S*-transferase	WP_045063292	49	(57)
24025	*styH*	9.5	6.3	5.0	4.8		*isoH*	1-hydroxy-2-glutathionyl-2-methyl-3-butene DH	WP_045063294	59	(57)
24030	*styG*	10.0	6.3	6.8	5.5	S3	*yfdE*	Acetyl-CoA:oxalate CoA-transferase	P76518	33	(100)
24035	*marR*	10.0	3.5	2.1	2.7		*marR*	regulatory protein	CAA52427	31	(101)
24040	*dsr*	9.1	4.7	8.5	4.8		*dsr*	Coenzyme A disulfide reductase	O58308	34	(102)
24045	*gshB*	8.9	4.9	5.7	3.8		*gshB*	Glutathione synthetase	P45480	50	(103)
24050	*gshA*	9.0	3.4	5.5	-2.2		*gshA*	Glutamate-cysteine ligase EgtA	P9WPK7	33	(104)

728 **Table 2.** (Continued)

ID	gene	A	M	Cyt	Mem		gene	description	accession	%	ref
24055	Hyp	7.8	8.5	NaNf	8.8	S2		-			
24060	Hyp	7.0	9.3	7.5	10.3			-			
24065	Hyp	6.6	9.3	8.8	10.3			-			
24070	Hyp	7.1	8.4	8.2	8.4			-			
24075	Hyp	6.8	9.5	7.9	8.2			-			
24080	Hyp	7.8	8.0	8.0	8.2			-			
24085	Hyp	9.2	10.7	5.8	6.2			-			
24090	Hyp	7.4	10.4	9.2	9.0			-	BAL04131	-	(13, 50)
24095	*styB*	8.9	9.4	11.2	8.5	S1	*styB*	StyB-SMO flavin oxidoreductase	BAL04130	82	(13, 50)
24100	*styA*	9.0	9.1	8.1	6.0		*styA*	StyA-SMO styrene monooxygenase	BAL04129	86	(13, 50)
18380	prmA	5.3	3.5	3.4	3.2	Chromosome	prmA	propane monooxygenase hydroxylase large subunit	BAD03956	96	(25)
18385	prmB	3.1	4.8	4.9	2.0		prmB	propane monooxygenase reductase	BAD03957	80	(25)
18390	prmC	4.1	4.0	3.7	2.4		prmC	propane monooxygenase hydroxylase small subunit	BAD03958	85	(25)
18395	prmD	4.1	4.3	4.7	4.4		prmD	propane monooxygenase coupling protein	BAD03959	94	(25)
18400		3.7	3.7	4.9	2.3			-			
18405		3.3	3.8	NaNf	1.7			-			
18410	adh	3.5	3.8	3.4	1.5		aldh1	alcohol dehydrogenase	BAD03962	88	(25)
18415	groL	4.4	3.7	3.5	1.3		*groL*	60 kDa chaperonin	P28598	52	(105)
14195	ahpD	7.1	3.2	4.7	4.5		*ahpD*	Alkyl hydroperoxide reductase AhpD	Q50441	74	(106)
14190	ahpC	7.7	4.9	4.1	2.5		*ahpC*	Alkyl hydroperoxide reductase subunit C	A0R1V9	86	(107)
14185	oxyR	2.7	5.1	1.2	2.6		*oxyR*	Probable hydrogen peroxide-inducible genes activator	Q9X5P2	53	(108)

729 Transcript abundance (A) and fold-change (M) as well as protein fold-change in cytosol (Cyt) and membrane fraction (Mem) is given as log2 ratio. NaNf – not detected
730 in the fructose proteome; NaN – not detected

731

1   **Table 3.** Plasmids used in this study

Plasmid	Relevant characteristic(s)	Source or reference
pET16bP	pET16b with additional multicloning site; allows synthesis of recombinant proteins with an N-terminal His$_{10}$-tag	U. Wehmeyer*
pEX-K2-pSGrA1	*GCWB2_24100* (1284-bp NdeI/NotI fragment) cloned into pEX-K2 vector	MWG Eurofins
pEX-K2-pSGrA2	*GCWB2_21620* (1359-bp NdeI/NotI fragment) cloned into pEX-K2 vector	MWG Eurofins
pEX-K2-pSGrD1	*GCWB2_23925* (1488-bp NdeI/NotI fragment) cloned into pEX-K2 vector	MWG Eurofins
pEX-K2-pSGrD2	*GCWB2_24010* (1437-bp NdeI/NotI fragment) cloned into pEX-K2 vector	MWG Eurofins
pSGrA1_P01	*GCWB2_24100* (1284-bp NdeI/NotI fragment) cloned into pET16bP	This study
pSGrA2_P01	*GCWB2_21620* (1359-bp NdeI/NotI fragment) cloned into pET16bP	This study
pSGrD1_P01	*GCWB2_23925* (1488-bp NdeI/NotI fragment) cloned into pET16bP	This study
pSGrD2_P01	*GCWB2_24010* (1437-bp NdeI/NotI fragment) cloned into pET16bP	This study

2   * personal communication

3

4